UNIVERSIDADE ESTADUAL DE CAMPINAS
FACULDADE DE ODONTOLOGIA DE PIRACICABA

GABRIELA DE ALENCAR PINTO MAGALHÃES

INCORPORAÇÃO DE UMA VITRO-CERÂMICA BIOATIVA EM CIMENTOS DE IONÔMERO DE VIDRO – ESTUDO EXPLORATÓRIO DAS PROPRIEDADES FÍSICO-MECÂNICAS E BIOLÓGICAS

INCORPORATION OF A GLASS-CERAMIC INTO GLASS IONOMER CEMENTS – AN EXPLORATORY STUDY OF THE PHYSIC-MECHANICAL AND BIOLOGICAL PROPERTIES

Piracicaba
2023

GABRIELA DE ALENCAR PINTO MAGALHÃES

INCORPORAÇÃO DE UMA VITRO-CERÂMICA BIOATIVA EM CIMENTOS DE IONÔMERO DE VIDRO – ESTUDO EXPLORATÓRIO DAS PROPRIEDADES FÍSICO-MECÂNICAS E BIOLÓGICAS

INCORPORATION OF A GLASS-CERAMIC INTO GLASS IONOMER CEMENTS – AN EXPLORATORY STUDY OF THE PHYSIC-MECHANICAL AND BIOLOGICAL PROPERTIES

Tese apresentada à Faculdade de Odontologia de Piracicaba da Universidade Estadual de Campinas como parte dos requisitos exigidos para a obtenção do título de Doutora em Odontologia, na Área de Odontopediatria.

Thesis presented to the Piracicaba Dental School of the University of Campinas in partial fulfillment of the requirements for the degree of Doctor in Dentistry, in Pediatric Dentistry area.

Orientadora: Profa. Dra. Regina Maria Puppin Rontani
Coorientadora: Profa. Dra. Fernanda Miori Pascon

ESTE EXEMPLAR CORRESPONDE À VERSÃO FINAL DA TESE DEFENDIDA PELA ALUNA GABRIELA DE ALENCAR PINTO MAGALHÃES E ORIENTADA PELA PROF. DRA. REGINA MARIA PUPPIN RONTANI.

Piracicaba-SP
2023

Ficha catalográfica
Universidade Estadual de Campinas
Biblioteca da Faculdade de Odontologia de Piracicaba
Marilene Girello - CRB 8/6159

M27i

Magalhães, Gabriela de Alencar Pinto, 1994-
Incorporação de uma vitro-cerâmica bioativa em cimentos de ionômero de vidro - estudo exploratório das propriedades físico-mecânicas e biológicas / Gabriela de Alencar Pinto Magalhães. – Piracicaba, SP : [s.n.], 2023.

Orientador: Regina Maria Puppin Rontani.
Coorientador: Fernanda Miori Pascon.
Tese (doutorado) – Universidade Estadual de Campinas, Faculdade de Odontologia de Piracicaba.

1. Cimentos de ionômeros de vidro. 2. Biomateriais. I. Puppin-Rontani, Regina Maria, 1959-. II. Pascon, Fernanda Miori, 1977-. III. Universidade Estadual de Campinas. Faculdade de Odontologia de Piracicaba. IV. Título.

Informações Complementares

Título em outro idioma: Incorporation of a glass-ceramic into glass ionomer cements - an exploratory study of the physic-mechanical and biological properties
Palavras-chave em inglês:
Glass ionomer cements
Biomaterials
Área de concentração: Odontopediatria
Titulação: Doutora em Odontologia
Banca examinadora:
Fernanda Miori Pascon [Coorientador]
Mário Alexandre Coelho Sinhoreti
Kamila Rosamilia Kantovitz
Américo Bortolazzo Correr
Marina Studart Alencar Borges
Data de defesa: 03-04-2023
Programa de Pós-Graduação: Odontologia

Identificação e informações acadêmicas do(a) aluno(a)
- ORCID do autor: https://orcid.org/0000-0002-7001-8850
- Currículo Lattes do autor: http://lattes.cnpq.br/8814403569329048

UNIVERSIDADE ESTADUAL DE CAMPINAS
Faculdade de Odontologia de Piracicaba

A Comissão Julgadora dos trabalhos de Defesa de Tese de Doutorado, em sessão pública realizada em 03 de abril de 2023, considerou a candidata GABRIELA DE ALENCAR PINTO MAGALHÃES aprovada.

PROFª. DRª. FERNANDA MIORI PASCON

PROFª. DRª. MARINA STUDART ALENCAR BORGES

PROFª. DRª. KAMILA ROSAMILIA KANTOVITZ

PROF. DR. MÁRIO ALEXANDRE COELHO SINHORETI

PROF. DR. AMERICO BORTOLAZZO CORRER

A Ata da defesa, assinada pelos membros da Comissão Examinadora, consta no SIGA/Sistema de Fluxo de Dissertação/Tese e na Secretaria do Programa da Unidade.

AGRADECIMENTOS

Agradeço à Deus, meu Senhor e criador, pela misericórdia em minha vida, e por ter me abençoado em todos os momentos, colocando sempre as pessoas certas, nos momentos certos em cada fase dessa jornada de amadurecimento pessoal e profissional.

Agradeço aos meus pais Ciro Gomes Magalhães e Mariêta de Alencar Pinto Goulart, por acreditarem em mim, e por ter sido minha fonte de amor e força. Aos meus irmãos; Antônio Moreira Magalhães Neto, por ser sinônimo de força e coragem, e me passar isso mesmo que à tantos quilômetros de distância. À minha irmã amada, Ana Beatriz de Alencar Pinto Magalhães, por todo amor e carinho vindos de seus abraços esmagadores. Ao irmão caçulinha, Ciro Gomes Magalhães Filho, pelo seu olhar doce e puro de criança, que me transmitiram ternura e esperança.

Faltam-me palavras para expressar a profunda gratidão e admiração pessoal e profissional ao meu namorado Rafael Rocha Pacheco. Além de ter sido o meu companheiro de vida, participou ativamente dessa jornada, me abrindo portas no exterior e me oferecendo sempre o que havia de melhor. Deus me agraciou com a sua presença do início ao fim desse ciclo, tão importante em minha vida. Muito obrigada por cada uma das muitas contribuições neste trabalho, e por todo amor e suporte dado mesmo à distância.

Agradeço a amizade, regada à muita diversão, momentos de desenvolvimento pessoal e profissional das amigas: May Anny A. Fraga, a quem recorri inúmeras vezes solicitando consultoria estatística e metodológica; Talita M. Carletti, Jéssica C. Reis e Rayanne Cunha Vieira. Compartilhamos muito além da casa, mas sim a própria vida.

Agradeço especialmente aqueles que foram imprescindíveis para a realização desse trabalho: Profa. Regina Maria Puppin Rontani, Rafael Rocha Pacheco, Edgar Dutra Zanotto, Marina Sousa Trevellin, Joshua Thomson, Cristine Smoczer e Laura Yang.

À minha orientadora Profa. Dra. Regina Maria Puppin Rontani. Obrigada pela orientação desde o mestrado, em Materiais Dentários, e por ter me apoiado a seguir com o Doutorado na Odontopediatria. Sou muito grata por todas as correções, conversas e oportunidades ao longo dessa jornada. Admiro a sua força, dinamismo e inteligência. Com certeza, levarei cada um de seus ensinamentos profissionais e pessoais no meu coração.

Ao Prof. Dr. Edgar Dutra Zanotto do Laboratório de Materiais Vítreos da Universidade Federal de São Carlos, por compartilhar sua ideia inicial e por contribuir fortemente com a realização da pesquisa através do compartilhamento de contatos, literatura e material.

À Profa. Dra. Marina Trevelin Souza pelo fornecimento do material, contribuições metodológicas, apoio prestado e disponibilidade todas as vezes que solicitei ajuda.

Aos Profs. Drs. Joshua Thomson e Cristine Smoczer, por terem me recebido na UDM – University of Detroit Mercy Shool of Dentistry entre setembro e dezembro de 2022. Agradeço pela disponibilidade em realizar os experimentos biológicos junto a mim, pela dedicação que tiveram com este trabalho. Sou grata por cada minuto que tivemos na bancada do laboratório, em reuniões de planejamento e discussões dos dados. Agradeço a técnica do laboratório de biomédicas da UDM Laura Yang, Ph.D, que sempre esteve me auxiliando e me ensinando as metodologias no laboratório. A vocês, fica a minha gratidão por todos os ensinamentos e momentos de convivência.

Aos membros avaliadores das bancas de qualificação I e II, que contribuíram ricamente para o melhoramento deste trabalho: Professores doutores Isaac Jordão de Souza Araújo, Gabriel Flores Abuna, Rafael Pino Vitti e Américo Bortolazzo Correr.

Agradeço pelas noções básicas e extremamente importantes para a realização dos experimentos, aos técnicos do Laboratório de Odontopediatria da FOP-Unicamp, Sr. Marcelo Correa Maistro; do Laboratório de Materiais Dentários Sr. Marcos Blanco Cangiani; e do Microscópio Eletrônico de Varredura, Sr. Adriano Luís Martins.

Gostaria de reconhecer o respeitável papel das professoras do PPGO-Odontopediatria, Profas. Dras. Carolina Stainer de Oliveira Alarcon, Fernanda Miori Pascon, Maria Beatriz Duarte Gavião, Marinês Nobre dos Santos Uchoa e Aline Rogéria Freire de Castilho. Obrigada por contribuírem ricamente com meu desenvolvimento através dos seminários, discussões de casos clínicos e experiências partilhadas na clínica de graduação e no plantão de urgência.

Agradeço em especial à Profa. Dra. Fernanda Miori Pascon, por assumir a banca examinadora da tese, como co-orientadora, no papel de presidente da banca.

Agradeço aos colegas do PPGO-Odontopediatria pelo prazer de ter partilhado essa jornada: Felipe Fabrício, Juliana Benine, Letícia Pereira, Carla Marinho, Camilla Beckman, Camila Marceliano, Willian Segatto, Patricia Vítor, Cinthia Arias e Cinthia Lopes, Carmem Bastos, Edith Camila, Carine Rabelo, Núbia Ribeiro e Ana Cecília.

Agradeço à Coordenadoria de Pós Graduação por todas as orientações e serviços prestados ao longo desta jornada.

Agradeço ao Conselho Nacional de Desenvolvimento Científico e Tecnológico (CNPQ) pela bolsa concedida (processo 141450/2020-7) durante este período.

O doutorado representa a possibilidade de dedicação intensa a um projeto que se acredita fazer a diferença para a sociedade. Mesmo sendo materializado em uma tese, seu aprendizado não cabe em um documento. Agradeço a todos que participaram direta e indiretamente deste projeto pessoal e profissional.

RESUMO

Os cimentos de polialcenoato de vidro ou Cimentos de Ionômero de Vidro (CIV), têm se mostrado os materiais mais apropriados para estar em contato com a Dentina Afetada por Cárie (DAC). Contudo, a baixa liberação de íons importantes para a remineralização da DAC demanda a exploração formulações de CIV's contendo vidros bioativos, para melhorar as propriedades mecânicas, antibacteriana e liberação iônica. Esse estudo tem por objetivo explorar o efeito da adição de uma vitrocerâmica bioativa (Biosilicato® 23,75Na_2O– 23,75CaO–48,5SiO_2 –4P_2O_5) nas propriedades físico-mecânicas e biológicas de um CIV restaurador convencional de baixa viscosidade (Maxxion R) e um de alta viscosidade (Fuji IX GP). O Biosilicato® foi incorporado em diferentes concentrações (5%, 10% e 15% P/P) aos diferentes CIVs. A caracterização da superfície (n=3) foi feita por MEV (n=3), EDS (n=3) e FTIR (n=1). Os tempos de presa e trabalho (T/P) (n=3), e a resistência à compressão (RC) (n=10) foram avaliados de acordo com a ISO 9917-1:2007. A liberação de íons foi determinada e quantificada por ICP-OES e por UV-Vis para Ca, Na, Al, Si, P, F (n=6). Para verificar a citotoxicidade, células tronco da papila apical (SCAP) foram expostas a eluatos desses cimentos (n=3 e relação área superficial/meio = 1,8 cm^2/mL) e analisadas 24 h após a exposição. A atividade antimicrobiana contra *Streptococcus mutans* (ATCC® 25175, NCTC 10449) foi analisada por contato direto do inóculo com o material por 2 h (n=5). Os dados foram submetidos aos testes de normalidade e lognormalidade de Shapiro-Wilk. ANOVA(one-way) e teste de Tukey foram aplicados nos dados dos tempos T/P, RC e liberação de íons. Os dados de citotoxicidade e atividade antimicrobiana foram submetidos ao teste de Kruskal-Wallis e de Dunn como teste post-hoc. Todos os testes estatísticos foram aplicados considerando alfa=5%. A análise das características de superfície foi feita por análise qualitativa. Os resultados mostraram que entre todos os grupos, aqueles com 5% (peso) de Biosilicato® apresentaram melhor qualidade superficial. Os dados de FTIR mostraram uma boa interação entre o Biosilicato® e a matriz do CIV. Apenas Maxxion com 5% de Biosilicato apresentou tempos de T/P comparável ao material original (p=0,7254 e p=0,5912). A RC foi mantida em todos os grupos Maxxion (p>0,0001) e diminuiu nos grupos experimentais Fuji (p<0,0001). A liberação de Na, Si, P e F foi significativamente aumentada para todos os grupos Maxxion e Fuji (p<0,0001). A citotoxicidade foi aumentada apenas para Maxxion com 5% e 10% de Biosilicato®. A

maior inibição do crescimento de *S.mutans* foi observada para Maxxion com 5% de Biosilicato® (menos de 100 UFC/mL), seguido de Maxxion com 10% de Biosilicato® (p=0,0053) e Maxxion sem a vitrocerâmica (p=0,0093). Maxxion R e Fuji IX apresentaram comportamentos diferentes quanto à incorporação do Biosilicato®, com o Maxxion R apresentando as maiores discrepâncias. Os impactos nas propriedades físico-mecânicas e biológicas foram diferentes dependendo do tipo do CIV, mas a liberação de íons terapêuticos foi aumentada para ambos os materiais.

Palavras-chave: Cimento de polialcenoato. Cimento de ionômero de vidro. Biomateriais. Cerâmica vítrea.

ABSTRACT

Glass Ionomer Cements (GIC), also known as glass polyalkenoate cements, are the most appropriates materials for to be in contact with Caries Affected Dentin (CAD). However, the low release of crucial ions for CAD remineralization in GICs necessitates the exploration of alternative formulations of GICs. The incorporation of bioactive glasses has been suggested as a means of enhancing the mechanical, antibacterial, and ion release properties of GICs. This study aims to explore the effect of adding a bioactive glass-ceramic (Biosilicate® $23.75Na_2O– 23.75CaO–48.5SiO_2 –4P_2O_5$) on the physical-mechanical and biological properties of a conventional (Maxxion R) and in a high viscosity (Fuji IX GP) GICs. Biosilicate® was incorporated by weight (5%, 10% and 15%) in the GICs. Surface characterization was performed by SEM (n = 3), EDS (n = 3) and FTIR (n = 1). Setting and working times (S/T) (n = 3), and compressive strength (CS) (n = 10) were evaluated according to ISO 9917-1:2007. Ion release was determined and quantified by ICP-OES and by UV-Vis for Ca, Na, Al, Si, P, F (n = 6). To verify cellular cytotoxicity, Stem Cells from Apical Papilla (SCAP) were exposed to eluates (n=3 and 1.8 cm^2/mL ratio) and analized 24h after exposure. Antimicrobial activity against *Streptococcus mutans* (ATCC® 25175, NCTC 10449) was analyzed by direct contact for 2 h (n=5). The data were submitted to normality and lognormality tests. One-way ANOVA and Tukey's test were applied to WT/ST, CS and ion release data. Cytotoxicity and antimicrobial activity data were submitted to the Kruskal-Wallis and Dunn tests as a post-hoc test. Among all groups, those with 5% of Biosilicate® showed better surface quality. The FTIR data showed a good interaction between Biosilicate® and the GIC matrix. Only Maxxion with 5% of Biosilicate® presented W/S times comparable to the original material (p=0.7254 and p=5912). CR was maintained in all Maxxion groups ($p > 0.0001$) and decreased in the experimental Fuji groups ($p<0.0001$). The release of Na, Si, P and F was significantly increased for all Maxxion and Fuji groups ($p<0.0001$). Cytotoxicity was increased only for Maxxion with 5% and 10% Biosilicate®. The greatest inhibition of *S.mutans* growth was observed for Maxxion with 5% Biosilicate® (less than 100 CFU/mL), followed by Maxxion with 10% Biosilicate® (p=0.0053) and Maxxion without the glass-ceramic (p=0.0093).The impacts of adding Biosilicate® into Maxxion and Fuji IX over its physical-mechanical and biological properties were different depending on the GIC, but the release of therapeutic ions was increased for both materials.

Keywords: Glass polyalkenoate cement. Glass ionomer cement. Glass ceramic. Bioactive glass. Antibacterial agents.

SUMÁRIO

1 INTRODUÇÃO

Os cimentos de polialcenoato de vidro, popularmente conhecidos Cimentos de Ionômero de Vidro (CIVs) são materiais restauradores amplamente utilizados, devido a capacidade de se aderir quimicamente ao dente, liberar fluoreto, apresentar coeficiente de expansão térmico similar ao da dentina e biocompatibilidade (1). São cimentos que podem ser considerados multiuso devido a vasta aplicabilidade, tais como: base e forramento de cavidades, restaurações provisórias e permanentes, selantes de fóssulas e fissuras, cimentação e para fixação de bráquetes ortodônticos (2).

Diferentes tipos de CIVs encontram-se comercialmente disponíveis, tais como cimentos de ionômero de vidro convencionais, fotopolimerizáveis ou híbridos. Os convencionais podem ser classificados de alta viscosidade ou de baixa viscosidade a depender da proporção de pó/líquido (P/L) e a quantidade de íons Ca^{+} e Al^{3+} (3). Os CIVs de baixa viscosidade apresentam uma proporção P/L de 1.5/1 (peso/peso), baixas propriedades mecânicas e são indicados para restaurações provisórias. Enquanto os CIVs de alta viscosidade, apresentam proporção P/L 3.6/1 (peso/peso), o que reflete em melhores propriedades mecânicas e indicações clínicas mais longevas, como restaurações permanentes em regiões de grande carga mastigatória (4).

Algumas limitações específicas desse material podem ser apresentadas dependendo do fabricante, como a sensibilidade a umidade durante os estágios iniciais da presa, alta suscetibilidade a variações nos tempos de trabalho e presa, baixa resistência ao desgaste, baixas propriedades mecânicas (5). Um CIV com finalidade restauradora deve apresentar resistência à compressão a partir de 100 MPa, adequada microdureza (70 KNH), resistência à erosão ácida (>0.17mm) de acordo com a ISO 9917-1:2007, o que não é atingido por grande parte dos CIVs comercialmente disponíveis (6). A liberação de flúor é uma das principais vantagens desse material, e varia de acordo com a marca e a proporção P/L do CIV (7). Entretanto, ainda não há evidência clara sobre o quanto de liberação de flúor pelos CIVs seria necessário para se obter benefício clínico (1).

A composição do pó e do líquido varia de acordo com o fabricante, e consequentemente as propriedades do material também (5, 6). Esses materiais passam por constante aprimoramento na composição, no tamanho das partículas de

vidro e nos tipos de ácidos empregados, o que lhes confere diferentes propriedades físicas e mecânicas, bem como clínicas (5, 8, 9). Entretanto, é comum que o pó de vidro seja composto por partículas de cálcio-fluoro-aluminossilicato e a fase líquida, por uma solução aquosa de poliácidos (1).

Os poliácidos (alquenóico) são homopolímeros ou copolímeros de monômeros de ácidos mono, di ou tri-carboxílicos insaturados, como ácido acrílico, ácido maleico, ácido itacônico e ácido 2-buteno1,2,3 tricarboxílico (10). A composição, o peso molecular e a arquitetura dos poliácidos influenciam diretamente na manipulação e nas propriedades mecânicas dos CIVs (10, 11, 12, 13). O ácido tartárico, por exemplo, é comumente co-polimerizado ao ácido acrílico, e atua como um acelerador que auxilia na extração de íons do vidro aluminossilicato e facilita sua ligação às cadeias de poliânions (14).

O CIV é resultado da reação de neutralização entre a solução aquosa de ácido polimérico (ácidos polialcenóicos / ácidos carboxílicos) e o pó de vidro de caráter básico (1). Os íons cálcio e sódio não fazem parte da rede tridimensional do vidro, porém encontram-se dispersos nesta rede. Por isso e pela natureza bivalente do cálcio (Ca^{2+}) e univalente do sódio (Na^{+}), essa reação inicia preferencialmente por esses elementos, formando carboxilato de cálcio (ou estrôncio) e carboxilato de sódio imediatamente (10, 15). A degradação do vidro continua pela hidrolização das ligações de aluminossilicato (Al-O-Si) da rede de vidro e liberando cátions de alumínio, formando ligações cruzadas com os grupos carboxilatos (carboxilato de alumínio), o que irá conferir boas propriedades mecânicas ao material (16, 17).

O cimento em si, resulta em uma quantidade substancial de partículas de vidro parcialmente reagidas, que atuam como carga de reforço na matriz polimérica. De acordo com a norma ISO 9917-1:2007, o tempo mínimo de trabalho para este tipo de material deve ser de 1,5 minutos e o tempo de presa de 6 minutos. O mecanismo de adesão química à estrutura dentária ocorre através da quelação dos íons Ca^{2+} do esmalte/dentina pelos grupamentos carboxílicos livres na matriz polimérica. Logo, o CIV deve ser aplicado na cavidade ainda enquanto apresenta grupos carboxílicos livres, caracterizado pelo brilho superficial da mistura, para garantir o benefício da adesão química ao dente (18).

O uso dos CIV’s tem sido amplamente defendidos em tratamentos minimamente invasivos, como na Remoção Seletiva de Cárie (RSC) e no Tratamento Restaurador Atraumático (ART) (19, 20). O ART foi originalmente desenvolvido para

cuidados preventivos em áreas que carecem de recursos, como eletricidade ou equipamentos de alta/baixa rotação. Nessa técnica, apenas instrumentos manuais são usados para remover o tecido cariado, tendo alta adesão pelos pacientes pediátricos, porque está associado à redução da dor, desconforto e evita a necessidade de anestesia local (5). Mesmo com as limitações estéticas e mecânicas do material, restaurações com esse material no substrato de dentina afetada por cárie, apresentaram taxa de sobrevivência similar à de restaurações em resina composta e em amálgama após 3 anos de observação (21, 22).

As características do remanescente cariado são desafiadoras para se manter a estabilidade da restauração, uma vez que este substrato apresenta alto teor de água, alto conteúdo bacteriológico, superfície irregular e baixas propriedades mecânicas, comparada ao tecido hígido (23). Porém, deve-se considerar que além do alto conteúdo bacteriológico presente na dentina remanescente, após o ART ou RSC, mesmo após o vedamento da cavidade, o tecido dentinário permanece em degradação durante um período de 3 meses, período máximo investigado até o presente momento (24).

Dessa forma, a busca contínua por melhorias na atividade antimicrobiana e nas propriedades mecânicas desses materiais têm ocorrido desde a sua concepção. Diferentes materiais com propriedades antimicrobianas têm sido incorporados aos CIV tais como: compostos naturais (25, 26) clorexidina e antibióticos (27, 28, 29, 30), nanotubos de dióxido de titânio (31) e nanopartículas de prata (32). No entanto, a incorporação de de tais aditivos têm reduzido a resistência à compressão e estendido o tempo de presa do CIV (26, 27), enquanto nanopartículas de titânio e prata têm demostrado que além de melhorarem o efeito antimicrobiano, melhoraram as propriedades mecânicas de CIVs de alta viscosidade (33, 34).

Além da busca pela melhoria da atividade antimicrobiana e das propriedades mecânicas, elevar a bioatividade desse material tem sido muito almejada para a remineralização da dentina afetada por cárie (35, 36). Nesse contexto, aditivos inorgânicos bioativos como hidroxiapatita (37, 38, 39, 40), fluorapatita (41) e biovidros (42) têm sido incorporados aos CIVs como possibilidade elevar a bioatividade e atuarem como partículas de reforço. Porém, no geral não promoveram melhora significativa na resistência a compressão e causaram aumento no tempo de presa (42, 43, 44) com exceção de algumas formulações de biovidros livres de sódio e contendo

alumínio que mostraram não afetar a presa e aumentaram as propriedades mecânicas (45).

Os biovidros ou vidros bioativos, têm sido amplamente utilizados nas diversas especialidades odontológicas, para regeneração óssea, capeamento pulpar, terapias endodônticas, tratamento da hipersensibilidade dentinária, remineralização de esmalte e de dentina, e, com isso, têm sido frequentemente incorporados aos materiais restauradores e sistemas adesivos (46). Larry L. Hench foi pioneiro no desenvolvimento do biovidro. Enquanto pretendia criar um material de enxerto que não causasse rejeição pelo hospedeiro, desenvolveu o Bioglass® 45S5, um vidro do sistema quaternário que interage e se adere aos tecidos vivos pela indução da formação de uma camada de apatita (47).

Desde então diferentes formulações foram investigadas. A composição básica dos biovidros pode conter de 40–52% SiO_2, 10–50% CaO e 10–35% Na_2O. Também podem estar presentes em alguns biovidros 2–8% P_2O_5, 0–25% CaF_2 e 0–10% B_2O_3 (32%). Quando em solução aquosa, o material é capaz de precipitar a patita e também de se aderir aos tecidos duros e moles sem rejeição (48).

Segundo Larry L. Hench, ocorrem basicamente cinco estágios que antecedem a precipitação da apatita quando em contato com o biovidro: (estágio 1) troca iônica entre a superfície do biovidro e o meio (aquoso/fluido corporal), havendo a substituição de íons alcalinos e alcalinos terrosos da estrutura do vidro por H^+ e H_3O^+; (estágio 2) o pH é elevado e ocorre a ruptura das ligações Si-O-Si, assim o silício é liberado no fluido em forma de silanóis, $[Si(OH)_4]$; (estágio 3) em pH<9,5, os grupos silanóis se condensam sobre a partícula do biovidro, formando uma camada de gel de sílica. A troca iônica continua ocorrendo nesta camada superficial, principalmente recrutando o íons Ca^{2+} e PO_4^{3-};(estágio 4) formação de uma camada de cálcio e fosfato amorfo sobre o gel de sílica. Com o aumento da espessura dessa nova camada inicia-se a cristalização da apatita carbonatada (estágio 5) (49).

Esses materiais agregam a funcionalidade bioativa (formação de apatita) e antimicrobiana devido a sua alcalinidade, por isso promovem a remineralização do esmalte e da dentina, e apresentam efeito antibacteriano contra os microorganismos envolvidos na atividade da lesão cariosa. No tecido dentinário, forma-se uma ligação entre as partículas do biovidro e a dentina (50). Isso ocorre devido a comprovada afinidade do biovidro pelo colágeno tipo I (51). Abuna et al. (52) incorporaram

nanopartículas de biovidro a um sistema adesivo, que *in vitro* resultou na redução da degradação enzimática e remineralização da dentina afetada por cárie.

Especificamente na dentina desmineralizada, a adição de biovidro ao CIV promoveu maior formação de fluorapatita na superfície da dentina, e não interferiu na resistência adesiva do CIV a esse substrato (53). Apesar de suas excelentes propriedades bioativas, as principais desvantagens dos vidros bioativos são a baixa resistência mecânica (54). Sabe-se que o método de processamento do biovidro impacta diretamente na capacidade de formação da apatita (55). A taxa de formação de hidroxiapatita carbonatada (HAC) *in vitro* diminui significativamente à medida que a fração de volume cristalizado aumenta, indicando que o ganho nas propriedades mecânicas, com a cristalização, implicará na diminuição da bioatividade (47, 56, 57, 58).

Nesse contexto, o Biosilicato® [23,75Na_2O– 23,75CaO–48,5SiO_2 –4P_2O_5 (% em peso)] é um material vitrocerâmico bioativo totalmente cristalino que pode ser obtido com uma (BS-1P) ou duas fases cristalinas (BS-2P): silicato de sódio-cálcio ($Na_2CaSi2O_6$) ou ambos $Na_2CaSi_2O_6$ e uma solução de sódio– fases de fosfato de cálcio ($NaCaPO_4$) (59). Essa vitrocerâmica apresenta índice de bioatividade maior que o da hidroxiapatita e 99,5% de cristalinidade (47), atingido por meio do processo de cristalização controlada (58). Assim, Biosilicato® exibe propriedades mecânicas distintas dos biovidros, apresentando-se mais tenaz na forma monolítica e maior usinabilidade (47).

Alguns trabalhos como o de Saran *et al* 2020, reportaram aumento significativo das propriedades mecânicas com a incorporação de 10% em peso de pós cerâmicos aos CIVs. A composição específica dos pós cerâmicos muitas vezes não é clara, porém sabe-se que o óxido de zircônia é um dos principais constituintes. Devido ao ganho substancial nas propriedades mecânicas, os CIVs contendo pós cerâmicos geralmente são conhecidos como “Zircômero” ou “Amálgama branco” (60). Nomenclatura esta, fortemente criticada, uma vez que por definição “amálgama” são ligas de mercúrio (61).

O Biosilicato® foi inicialmente idealizado como um material bioativo para a utilização no tratamento da hipersensibilidade dentinária, e mostrou-se efetivo (62). Desde então, ampliaram-se as aplicações do material, foram realizados estudos *in vitro* e *in vivo,* mostrando significativa indução na osteogênese em culturas celulares

(63), materiais para proteção pulpar (64), na osseointegração de implantes (65) e na redução da desmineralização do esmalte causada pelo clareamento dental (62, 64).

O efeito antimicrobiano do Biosilicato® também é uma grande vantagem ao se considerar sua incorporação ao CIV. A vitrocerâmica mostrou-se efetiva quando testada em contato direto com 23 patógenos aeróbicos e anaeróbicos relacionados à cárie e à infecções endodônticas (66). A atividade antibacteriana do Biosilicato® se dá pela alteração no pH, que em meio aquoso aumenta de 5,0 para 8,7, em 35 minutos. Essa mudança promove significativa alteração no meio osmótico, sendo prejudicial aos microorganismos. A alcalinização do meio pode inativar algumas enzimas produzidas pelas bactérias (63), e a despolarização da membrana celular impactará nos processos do metabolismo celular, como a falta de ATP, e no transporte de nutrientes (67, 68). Contudo, essa vitrocerâmica ainda não foi incorporada aos CIVs.

A adição do Biosilicato® ao CIV representa uma possibilidade de melhorar o potencial de remineralização da dentina, pelo aumento na liberação de íons terapêuticos que também podem atuar no efeito antimicrobiano. Nesse contexto, o Biosilicato® foi incorporado em peso, em concentrações 5,10, e 15% aos dois tipos de CIVs, sendo um CIV convencional de baixa viscosidade (Maxxion R) e o outro de alta viscosidade (Fuji X GP). Dessa forma, o objetivo deste trabalho é investigar o efeito da adição de Biosilicato® nas propriedades físico-mecânicas, liberação de íons, citotoxicidade e atividade antimicrobiana contra *Streptococcus mutans*. As hipóteses são: a adição de diferentes concentrações de Biosilicato® aos CIVs impacta o tempo de presa e o comportamento mecânico (I); Biosilicato® aumenta a liberação de íons nos CIVs (II); diminui a citotoxicidade (III) e eleva a atividade antimicrobiana (IV).

2 ARTIGO: *Effect of Biosilicate® addition on the physical-mechanical and biological properties of dental glass ionomer cements.*

Gabriela de A. P. Magalhães [1], Joshua J. Thomson [2], Cristine Smoczer [2], Laura Young [2], Adaias O. Matos [3], Rafael R. Pacheco [4], Marina T. Souza[5], Edgar D. Zanotto[5] and Regina M. Puppin-Rontani [1]*

[1] Department of Health Sciences and Pediatric Dentistry, Pediatric Division, Piracicaba Dental School, UNICAMP, State University of Campinas, Piracicaba, SP, Brazil; gabrielaapmag@gmail.com
[2] Division of Integrated Biomedical Sciences, University of Detroit Mercy School of Dentistry, Detroit, MI, USA
[3] Division of Clinical Essentials and Simulation, University of Detroit Mercy School of Dentistry, Detroit, MI, USA
[4] Department of Restorative Sciences, Associate Professor and Section Director of Dental Materials, Dental College of Georgia at Augusta University, Augusta, GA, USA; rapacheco@augusta.edu
[5] Vitreous Materials Laboratory, Department of Materials Engineering, Center for Research, Education and Technology in Vitreous Materials (CeRTEV), Federal University of São Carlos (UFSCar), SP, Brazil
* Correspondence: rmpuppin@unicamp.br (R.PR)

Abstract: This study investigated the influence of Biosilicate® on the physico-mechanical and biological properties of glass ionomer cements (GIC). This bioactive glass ceramic ($23{,}75Na_2O– 23{,}75CaO–48{,}5SiO_2 –4P_2O_5$) was incorporated by weight (5%, 10%, or 15%) into commercially available GICs (Maxxion R and Fuji IX GP). Surface characterization was made by SEM (n = 3), EDS (n = 3), and FTIR (n = 1). Setting and working (S/W time) times (n = 3) and compressive strength (CS) were analyzed (n = 10) according to ISO 9917-1:2007. Ion release (n = 6) was determined and quantified by ICP OES and by UV-Vis for Ca, Na, Al, Si, P, F. To verify cell cytotoxicity, stem cells from the apical papilla (SCAP) were exposed to eluates (n = 3 and ratio 1.8 cm^2/mL) and analyzed 24h post-exposure. Antimicrobial activity against *Streptococcus mutans* (ATCC 25175, NCTC 10449) was analyzed by direct contact of 2h (n = 5). Data were submitted to normality and lognormality tests. One-way ANOVA and Tukey's test were applied for working and setting time, compressive strength, and ion release data. Data from cytotoxicity and antimicrobial activity were submitted to Kruskal-Wallis' test, and Dunn's as a post-hoc tests ($\alpha = 0.05$). Among all experimental groups, only those with 5% (wt) of Biosilicate® showed better surface property.Only M5% showed a comparable W/S time to the original material ($p = 0.7254$ and $p = 0.5912$). CS was maintained for all Maxxion R groups ($p > 0.0001$) and declined for

Fuji IX experimental groups ($p < 0.0001$). The Na, Si, P, and F ion releases were significatively increased for all Maxxion R and Fuji IX groups ($p < 0.0001$). Cytotoxicity was increased only for Maxxion R with 5% and 10% of Biosilicate®. A higher inhibition of *S.mutans* growth was observed for Maxxion R with 5% of Biosilicate® (less than 100 CFU/mL), followed by Maxxion R with 10% of Biosilicate® ($p = 0.0053$) and Maxxion R without the glass ceramic ($p = 0.0093$). Maxxion R and Fuji IX presented different behavior regarding Biosilicate® incorporation. The impacts on physico-mechanical and biological properties were different depending on the GIC, but therapeutic ion release was increased for both materials.

Keywords: glass ceramic; Biosilicate®; glass ionomer cement; ion release; bioactivity; antimicrobial; biocompatibility.

1. Introduction

Glass-ionomer cements (GICs) have been extensively employed as the material of choice for some minimally invasive dental procedures, such as atraumatic restorative treatment (ART) [1,2], demonstrating high durability and good clinical performance over several years [3]. Fluoride release, chemical adhesion to tooth, biocompatibility, and a thermal expansion coefficient close to that of dentine are well-known beneficial properties of GICs. [4]. The normal setting reaction of GIC results from the neutralization of an aqueous polymeric acid solution and a glass powder [5]. This reaction initially produces calcium polyacrylate (or strontium polyacrylate), followed by aluminum polyacrylate [6]. A significant amount of unreacted glass particles serves as reinforcing fillers in the polymeric matrix. The setting reaction typically lasts between 2 and 6 minutes [7].

The fluoride release from these materials, which provides an anti-cariogenic effect by inhibiting plaque formation [8-11], is insufficient to remineralize remaining caries-affected dentin after an ART procedure [4]. Since their introduction, GICs have undergone several improvements to the glass particle and polyacids used [4,12,13]. Bioactive materials such as hydroxyapatite, chitosan, bioglass, and even processed bovine dentin have been incorporated into GIC [14]. These bioactive materials have been studied to develop a restorative material that can provide remineralization, antimicrobial activity, and chemical interaction to restore challenging cavities, such as dentin affected by caries in deep caries lesions and cervical lesions [15,16].

BAG (Bioactive Glasses) was invented by Dr. Larry Hench in 1969 [21]. BAG incorporated into GICs have demonstrated the capability of inducing dentin remineralization [17-20]. Despite their excellent bioactive properties, bioactive glasses present low mechanical properties [22], for that reason bioactive glass ceramics have been created to overcome BAG's poor mechanical properties. However, as the crystallized volume fraction increases, the rate of apatite formation in vitro decreases significantly. The crystallization of this glass rendered it an inert substance.

Within this context Biosilicate® (BioS $23{,}75Na_2O$– $23{,}75CaO$–$48{,}5SiO_2$ – $4P_2O_5$) is a fully crystalline bioactive glass-ceramic that can be obtained with one (BS-1P) or two crystalline phases (BS-2P): sodium–calcium silicate ($Na_2CaSi_2O_6$) or both $Na_2CaSi_2O_6$ and a sodium-calcium phosphate ($NaCaPO_4$) phases [23]. Biosilicate®, on the other hand, is a type of bioactive glass ceramic produced by controlled crystallization, which allows leads to high crystallinity (higher mechanical properties)

without compromising its bioactivity [24]. This material is highly bioactive, osteoconductive, osteoinductive, non-cytotoxic and non-genotoxic, and it shows antibacterial properties. [23]. Biosilicate® has been used successfully for medical and dental applications, such as the treatment of dentine hypersensitivity [25], enamel remineralization agent [26], and antimicrobial agent in intracanal pastes [27], over the past two decades. Biosilicate® is a fully crystalline bioactive glass ceramic; therefore, it may be possible to incorporate it into GICs to increase their bioactivity and therapeutic ion release without compromising their mechanical properties.

The primary objective of this study is to investigate the effects of incorporating Biosilicate® into commercially available conventional and high viscosity GIC on setting behavior, mechanical properties, ion release, cytotoxicity, and antimicrobial activity against *S.mutans*. Thus, the research hypotheses tested are: (I) Different concentrations of Biosilicate® into GIC will affect their setting time and mechanical properties; (II) Biosilicate® incorporation into GIC increases their ion release, (III) cytotoxicity, (IV) and antimicrobial activity.

2. Materials and Methods

2.1. Formulation of experimental restorative materials and group assignments

Biosilicate® microparticles (D50= 5 μm) were synthesized by melting followed by a heat treatment, as described by Martins et al., (2011). Two glass ionomer cements were investigated: Maxxion R (FGM, Joinville, Santa Catarina, Brazil) and Fuji XI GP GC Corporation, Tokyo, Japan). Table 1 shows the manufacturers and compositions of the materials used in the study. Biosilicate® and the powders portions of each GIC were weighed using a 0.1mg analytical balance (Chyo Balance JK 180; Chyo Corp., Tokyo, Japan). Then, Biosilicate® was manually incorporated into Maxxion R and Fuji IX powders in concentrations of 5, 10, or 15% by weight. Table 2 shows the group distributions, formulations, and powder/liquid (P/L) ratios used on this study. Maxxion R (M0%) and Fuji IX (F0%) without Biosilicate® were used as control groups. M0% and F0% were manipulated following each GIC manufacturer's instructions. For experimental groups F5%, F10%, and F15%, the P/L ratio was 1.8/1 (wt/wt) to improve handling conditions (when touched or drawn apart, these cements formed strings/fibrils that prevented proper handling). The P/L ratio for Maxxion R groups was kept as 1.5/1 (wt/wt).

Table 1. Manufacturers and composition of the materials used.

Material (manufacturers)	Composition
Biosilicate® (LaMaV-CeRTEV, São Carlos, SP, Brazil)	23,75Na_2O– 23,75CaO–48,5SiO_2 –4P_2O_5 (%wt), microparticles (D_{50}=5 μm).
Maxxion R, Shade A2 (FGM, Joinville, Santa Catarina, Brazil)	Powder: aluminofluorosilicate glass and calcium fluoride (10 g). Liquid: polycarboxylic acid, tartaric acid, and water (8 g).
Fuji IX GP, Shade A2 (GC Corporation, Tokyo, Japan – authorized by South America GC, SP, Brazil)	Powder: aluminofluorosilicate glass, polyacrilic acid. Liquid (4 mL): polyacrylic acid, water.

Table 2. Groups of experimental formulations by %wt and P/L ratios.

Groups	Formulations (% wt)	Ratio P:L (wt/wt)
M0%	100% Maxxion R	1.5/1
M5%	95% Maxxion R + 5% Biosilicate®	1.5/1
M10%	90% Maxxion R + 10% Biosilicate®	1.5/1
M15%	85% Maxxion R + 15% Biosilicate®	1.5/1
F0%	100% Fuji IX	3.6/1
F5%	95% Fuji IX + 5% Biosilicate®	1.8/1
F10%	90% Fuji IX + 10% Biosilicate®	1.8/1
F15%	85% Fuji IX + 15% Biosilicate®	1.8/1

2.2. Scanning Electronic Microscopy (SEM) and Energy-dispersive X-ray Spectroscopy (EDS)

The powders of each material (Fuji IX GP, Maxxion R, and Biosilicate®) were individually applied onto a carbon-tape mounted on plastic stubs using a plastic rod, and sputter-coated with gold (MED 010, Balzers, Liechtenstein) [28] to evaluate particle morphology. In addition, cylindrical molds (4.0 mm in diameter and 3.0mm in height) were fabricated. The cements were manipulated, inserted into the molds (n=3), and stored for 24h in relative humidity (100%). Following, the cylindrical specimens were split-off using a chisel and a hammer, finished and polished using #320 and #400 sandpaper with 99° ethanol, and stored for 24 h in a desiccator (Pyrex, São Paulo, SP,

Brazil) at 37°C. The specimens were mounted on the stubs, as previously described. A Scanning Electron Microscope was used (JSM-5600LV; Jeol, Tokyo Japan) and images were taken in magnifications of 1,000x, 5,000x, operating at 15 kV, ray width 25–30 nm, and working distance of 10–15 mm. Energy-dispersive x-ray spectroscopy (EDS) was performed to qualitatively estimate the amount of ions (Ca, P, Si, Al, Na, F) on the cross-section (as previously described) of the cylindrical specimens (n=3). The specimens were fixed on a carbon tape over a plastic stub, coated with carbon (MED 010, Baltec), and analyzed using 15 kV, working distance of 10 mm, spot size of 25 mm, and ×500 magnification. The images obtained in the SEM were used for qualitative analysis of the GIC surfaces, as well as the spectra obtained by the EDS evaluation.

2.3. Fourier Transform Infrared spectroscopy (FTIR)

To investigate GICs setting dynamics FTIR spectra were collected over time (n=1). The cements were mixed, immediately placed and kept in the spectrometer, obtaining curves after 1, 5, and 60 minutes [29]. The analysis was performed with a spectral resolution of 4 cm^{-1} in the region between 4000 to 400 cm^{-1} (Perkin Elmer, Spectrum GX. DE), though only the spectral range of interest (1800 to 900 cm^{-1}) was represented. FTIR spectra were baseline-normalized using a specific software (Spectragryph Software, Germany, version 2.16.1) and plotted in a statistical software (GraphPad, Prism, version 9.5.0). The peaks of interest were searched in the range of 1700 to 1715 cm^{-1} for poly-carboxylic acid and 1400 to 1640 cm^{-1} for poly-carboxylates salts [29-32].

2.4. Working and setting time

The working and setting times of evaluated GICs were measured by using Gilmore needles [33,34], n = 3. The cements were mixed and placed in metallic molds of 8.00 mm x 10.00 mm x 5.00 mm, on top of an aluminum foil. A large diameter needle (2.12 mm) with a weight of 113 g was applied and the working time was determined as soon as the needle no longer indented the surface. Then, a small diameter needle (1.06 mm) with 453.6 g of mass was positioned perpendicularly to the cement surface for 5 s. The indentations were repeated every 30 s in different spots until the needle failed to make a completely circular indentation, determining the setting time and it was obtained in seconds.

2.5. Compressive Strength (CS)

Eighty (80) cylindrical specimens (n=10) were prepared according to ISO 9917-1:2007 using custom silicone molds (4.00 mm in diameter and 6.00 mm in height). Cements were mixed and placed into molds between two glass slides protected by a transparent polyester film (Mylar®). Specimens were removed from the molds after 30 min and stored in 100% relative humidity in an incubator at 37ºC for 24 h. The tests were carried out at a speed of 0.75 mm/min under and 50 N/min load using a universal testing machine (Model 5544, Instron, Canton, MA, USA). The compressive strength (CS) was calculated (MPa) according to the formula:

$$Cs = \frac{4p}{\pi . D^2}$$

where *p* represents the load (Newton) exerted by the load cell until the sample failure, and *D* is the diameter of each specimen (mm), measured using a digital caliper (Mitutoyo, Japan).

2.6 Ion release by Inductively Coupled Plasma Optical Emission Spectrometry (ICP OES) and Ultraviolet-Visible Spectrometry (UV-Vis)

Forty-eight (48) cylindrical specimens (n=6) were made as previously described for CS and stored in an incubator at 37 °C for 1 h. The specimens were removed from the molds and placed in 20 mL of deionized water (DI) in plastic tubes (surface area/mL, 1 cm^2 /mL) [35]. The determination of Ca, Na, Al, Si, P and F ions in eluates were made using an Inductively Coupled Plasma Optical Emission Spectrometry (ICP OES), using iCAP 6000 (Thermo Fischer Scientific, Madison, WI, USA) and Ultraviolet-Visible Spectrometry, Uv-Vis. Quantifying and detection limits were respectively 0.050 and 0.015 ppm for Ca, Na, Al, Si, and P ion. Ultraviolet-Visible Spectrometry (UV-Vis) (DR/2500, HACH, Ames, Iowa, USA) was used to determine F ion release, according to Standard Methods for the Examination of Water and Wastewater (SMWW) – 4500 – F^- D. – SPANDNS. To quantify and detect F ions the limits considered were 0.100 and 0.030 ppm, respectively. To calculate the cumulative concentration of the

respective ions, the limit values of quantification and detection of the analysis methods used were normalized.

2.7 GIC cytotoxicity

The cytotoxicity was measured as part of the biocompatibility assessment. Twenty-four specimens (n=3) of 5.00 mm in diameter and 1.00 mm in thickness were made using polyvinylsiloxane (PVS) molds and allowed to set for 1 h at 37°C. Subsequently, specimens were added to 300 µL of cell culture media for 24 h at 37°C (surface area/mL was 1.8 cm^2/mL) [36]. The Promega CellTox™ Green assay was performed to assess the cytotoxicity of GICs on Stem Cells from Apical Papilla – SCAP, RP-89 cell line (donated by University of Texas Health Science Center Dental School, San Antonio, TX, USA). Cells were seeded at 10,000 cells/well in a black opaque-walled 96-well plate and maintained in α-MEM (Gibco, Grand Island, NY) supplemented with 10% fetal bovine serum (Gemini, West Sacramento, CA), 1% L-glutamine and 1% penicillin/ streptomycin (Sigma-Aldrich, St Louis, MO) at 37°C and 5% CO_2. After 24 h, the cell culture media was replaced by GIC-conditioned media. Cytotoxicity was evaluated by using the Promega CellTox Green® assay at 24 h post-exposure as per the manufacturer protocol. Fluorescence was read on a Spark® multimode microplate reader (Tecan, USA) with excitation/emission wavelengths of 485 nm / 520 nm. Cell exposed to the provided lysis buffer were considered positive control, while cells incubated in cell culture media alone were the negative control. Data were reported as percentage of dead cells in a population, relative to the positive control set arbitrarily to 100%.

2.8 Antimicrobial activity – Direct contact with disk surfaces

Forty specimens (n=5) of 15.00 mm in diameter and 1.00 mm in thickness were made using custom PVS molds. After 1 h setting at 37°C, each specimen was placed into a well of a 6-well plate and sterilized under UV light for 20 minutes per side. *Streptococcus mutans* Clarke (ATCC 25175, NCTC 10449) was inoculated in BHI broth (BD Difco™, Becton, Dickinson, and Company, Sparks, Maryland, USA) and incubated at 35°C ± 2°C supplemented with 5% CO_2 for 24 h. Then, the overnight inoculum was centrifuged and resuspended to an optical density at 600 nm (OD_{600}) =

1.0, approximately 1 × 10^9 colony-forming units/ml (CFU/ml) in dilute BHI (1:500 BHI in sterile DI water). Bacterial suspension was diluted 100-fold and 50 µL of the diluted bacterial suspension was added to each specimen surface (approximately 5.0 x 10^5 CFU/specimen). Then, a UV-sterilized plastic coverslip (15.00 mm in diameter) was aseptically placed onto each disk and incubated at 100% relative humidity at 25°C ± 2°C. After 2 h of direct contact, 950 µL of sterile phosphate-buffered saline (PBS) was added to each specimen/well and the plate was placed on an orbital shaker (Orbit™ 1000, Labnet International Inc., Edison, New Jersey, USA) at 150 rpm for 2 min to remove bacteria from the surface of the specimen. Then, liquid from each well (1 mL) was collected and serially diluted for plating onto BHI agar. Plates were incubated in a aerobic environment (tissue culture incubation conditions) at 35°C ± 2°C for 48h. The colonies formed were counted using a Colony Counter (Bantex® 920A, American Bantex Corp, Burlingame, California, USA) and CFU remaining after surface exposure was calculated.

2.9 Data analysis

Statistical analysis was performed using GraphPad Prism 9 version 9.5.0 (November 2022). The Shapiro-Wilk test was utilized to examine the normality and lognormality of cell viability data with a significance level of 0.05. The Compressive Strength and Ion Release presented normal distribution, and the data were submitted to one-way ANOVA followed by a Tukey's multiple comparisons test. Due to the non-normal distribution of cell viability and antimicrobial data ($p < 0.05$), Kruskal-Wallis' test was recommended to detect differences in group medians ($p < 0.05$). The multiple comparisons post-hoc test developed by Dunn was used to identify differences between experimental groups.

3. Results

3.1. SEM and EDS analyses

Figure 1 depicts the particle shape and size of Fuji IX (Figure 1A), Maxxion R (Figure 1B), and Biosilicate® (Figure 1C). All materials were observed to have non-uniform particle sizes. As seen in SEM images, Fuji IX particles are more sphere-like (octahedron shape), whereas Maxxion R particles have sharp edges (hexahedron shape). Small Biosilicate® particles have a sphere-like form and are clustered on large

particles (hexahedron shape), indicating a greater particle size distribution. The particles were categorized based on their shapes [37].

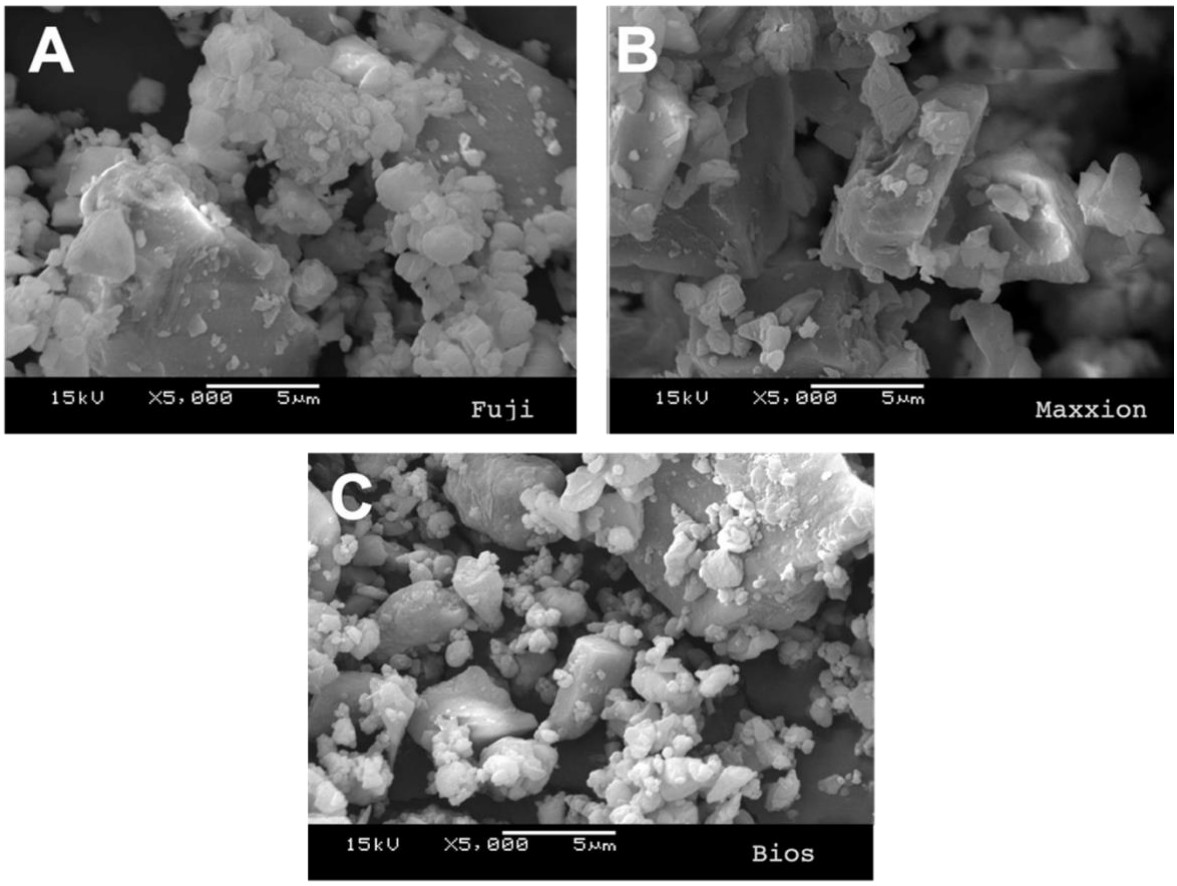

Figure 1. SEM analysis of GIC and Biosilicate® powders. A: Fuji IX GP; B: Maxxion R; C: Biosilicate®.

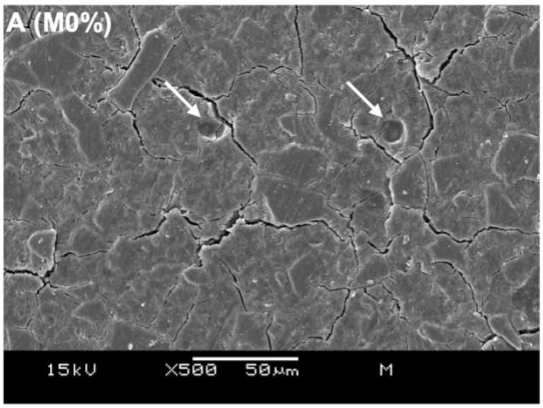
A (M0%)
15kV X500 50µm M

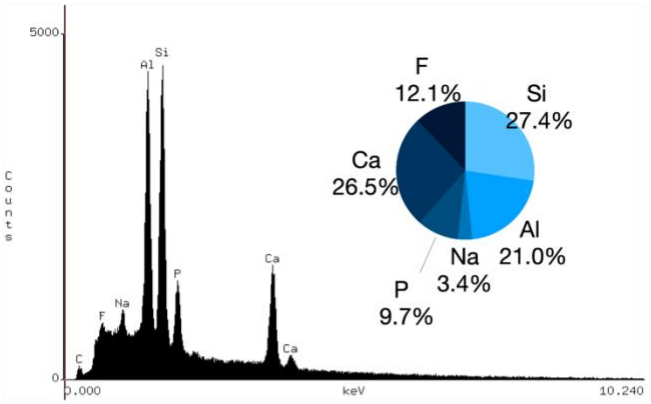
5000
0
Counts
C
F
Na
Al
Si
P
Ca
Ca
0.000
keV
10.240
F 12.1%
Si 27.4%
Ca 26.5%
Al 21.0%
Na 3.4%
P 9.7%

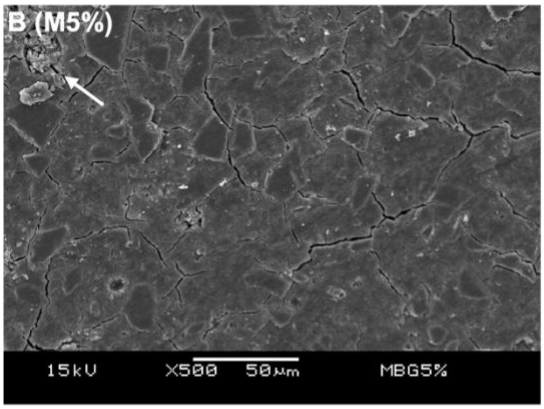
B (M5%)
15kV X500 50µm MBG5%

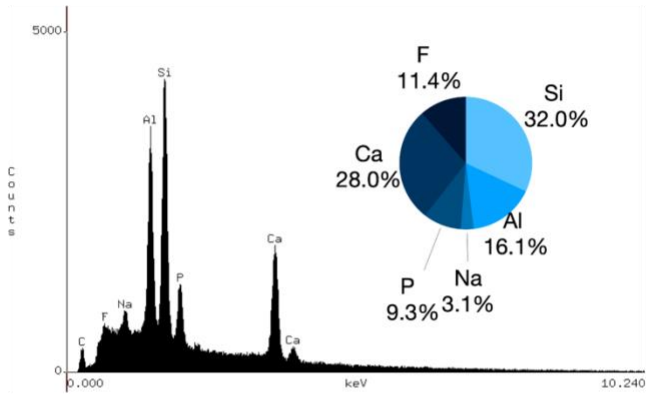
5000
0
Counts
C
F
Na
Al
Si
P
Ca
Ca
0.000
keV
10.240
F 11.4%
Si 32.0%
Ca 28.0%
Al 16.1%
P 9.3%
Na 3.1%

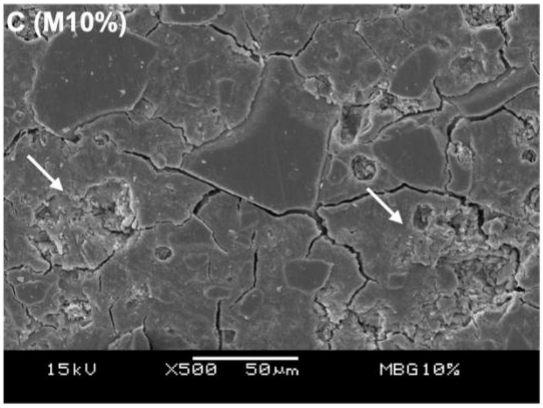
C (M10%)
15kV X500 50µm MBG10%

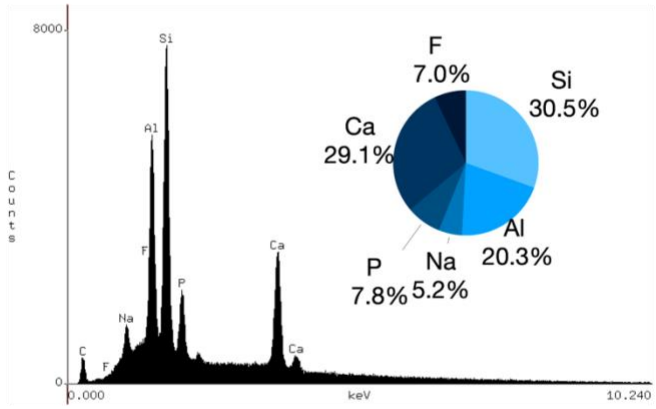
8000
0
Counts
C
F
Na
Al
Si
P
Ca
Ca
0.000
keV
10.240
F 7.0%
Si 30.5%
Ca 29.1%
Al 20.3%
P 7.8%
Na 5.2%

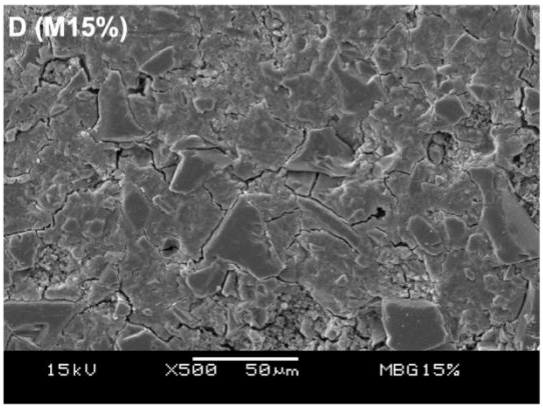
D (M15%)
15kV X500 50µm MBG15%

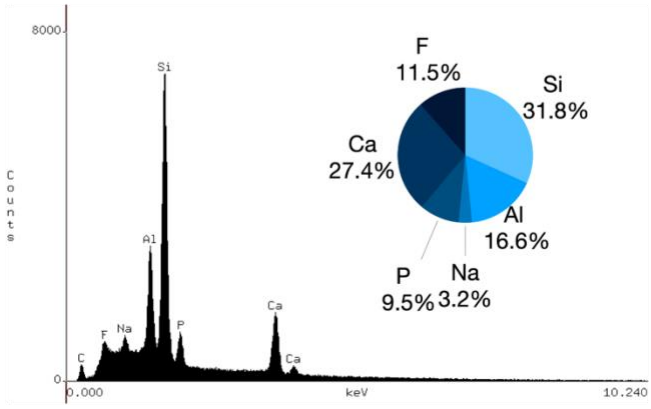
8000
0
Counts
C
F
Na
Al
Si
P
Ca
Ca
0.000
keV
10.240
F 11.5%
Si 31.8%
Ca 27.4%
Al 16.6%
P 9.5%
Na 3.2%

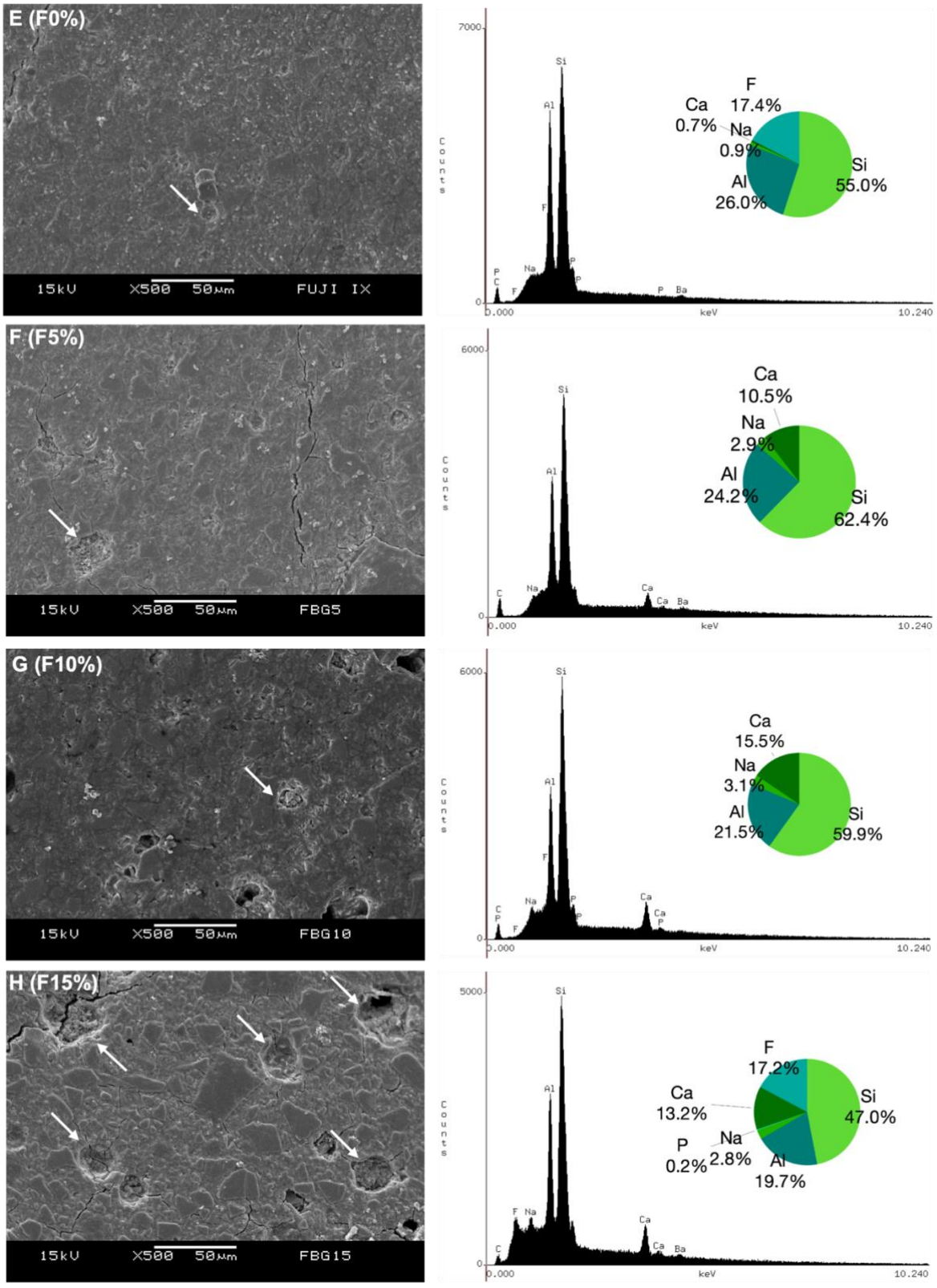

Figure 2. Representative SEM micrographs from each group and EDS histogram of the main ions present on their internal surface (%wt) as determined by EDS. A-D: Maxxion R groups; E-H: Fuji IX groups.

Figure 2 depicts the surface morphology of specimens. All groups presented crack lines on their specimens' surfaces. However, Fuji IX groups were observed to have smoother surfaces, with less apparent porosity and fewer cracks than Maxxion R groups. All experimental cements exhibited clusters of unreacted small particles whose number increased with increasing Biosilicate® concentration (white arrows). Figure 2 also shows histograms and the EDS spectra (%wt): calcium (Ca), phosphorus (P), silicon (Si), aluminum (Al), sodium (Na), fluorine (F), in the final mixture for each cement.

3.1. FTIR

Figure 3 depicts the FTIR spectrum of cements at 1, 5, and 60 minutes after initial mixing. Data from the FTIR of all samples showed absorption bands in 1715, 1560, 1455, 1415, 1170, 1060, and 940 cm^{-1}. As the materials set, the intensity of the –COOH groups of polyacrylic acid (1715 cm^{-1}) decreases and reorganizes as COO- (polycarboxylate salts) groups (1400–1640 cm^{-1}), as indicated by the dashed lines. The loading graph reveals that these two bands vary significantly at 1, 5, and 60 minutes of setting. The neutralization reaction appeared at 1170 (Si-O), 940 (O–H) cm^{-1}, and with the silica gel (Si-OH) at 1060 cm^{-1}.

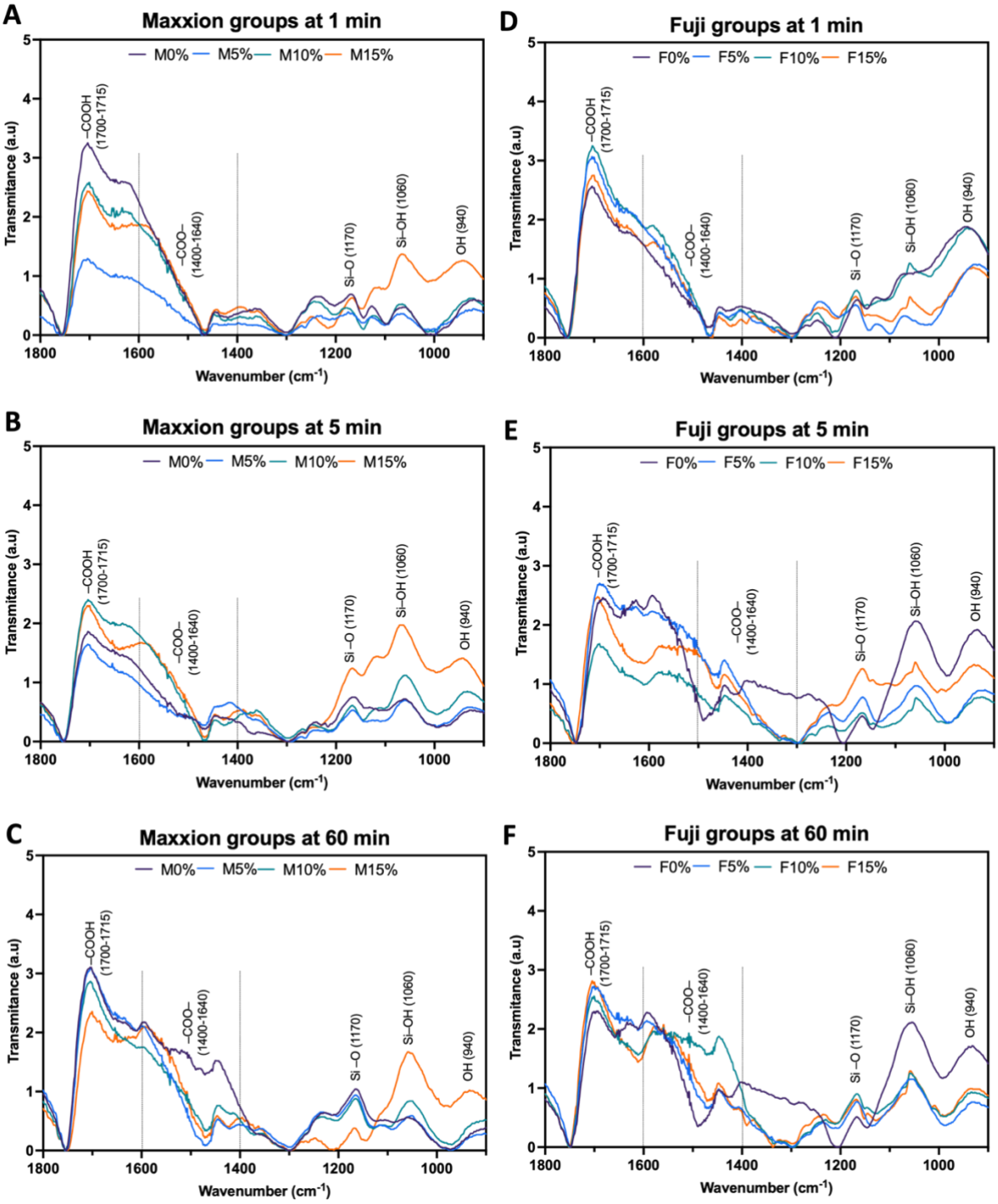

Figure 3. Data from the FTIR of Maxxion R (A, B, and C) and Fuji IX groups (D, E, and F) at 1, 5, and 60 minutes.

3.3. Setting and Working time

Figure 4 shows the working and setting times for cements. M10% exhibited the longest working time for Maxxion R (Figures 4A and 4B), whereas M15% exhibited the shortest. M0% and M5% showed similar working and setting time, and no significant

differences were found (p = 0.7254 and p = 5912). There was no significant difference in working time between M5% and M10% (p = 0.1314). M15% working and setting times were significantly shorter than M0% (p = 0.0072 and p = 0.0071). All experimental groups for Fuji IX (Figures 4C and 4D) had significantly longer working and setting times than F0%. F5% had the longest working time, followed by F15% and F10%, while F0% had the shortest. F15% did not differ significantly from F5% (p = 0.1150) and F10% (p = 0.9017) regarding working time. However, F15% had the shortest setting time, followed by F5% and F10%, which were similar (p = 0.8043).

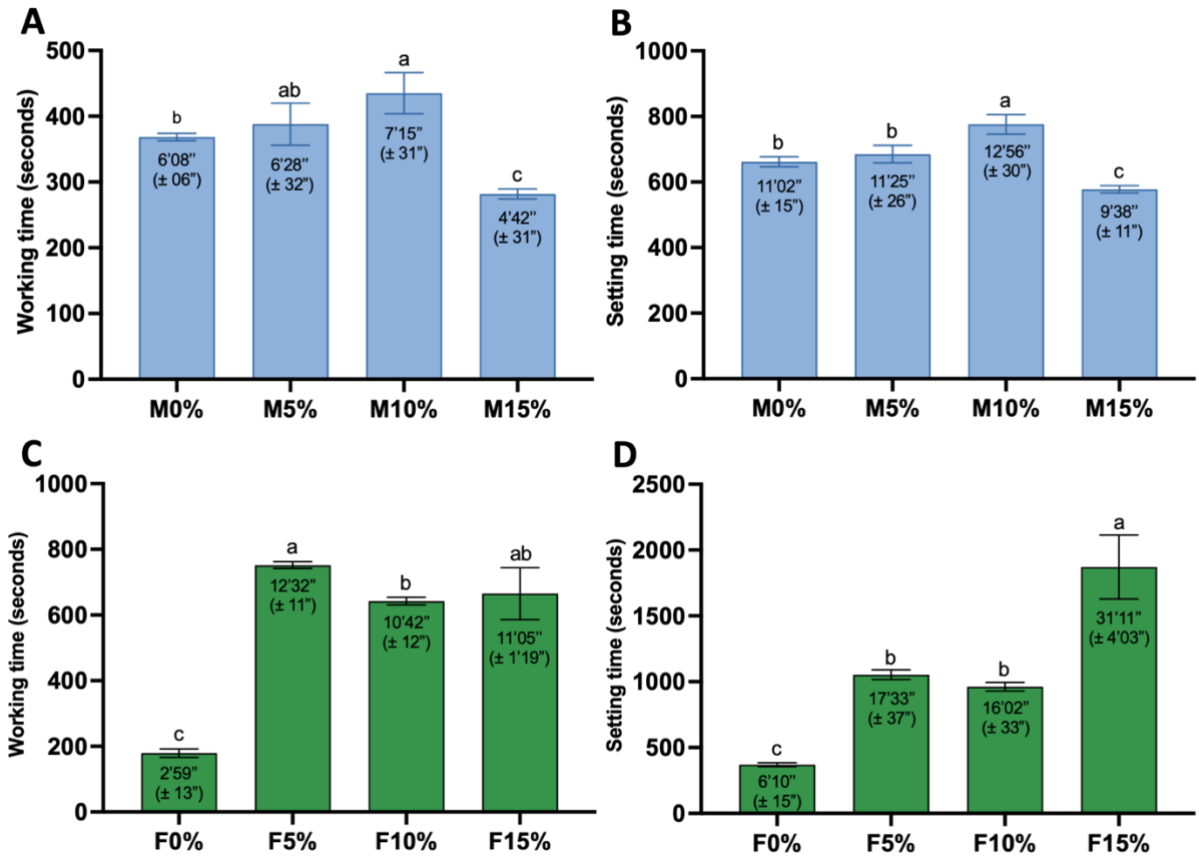

Figure 4. Working and setting times of GICs, in seconds. Error bars represent standard deviations. One-way ANOVA and Tukey's, performed separately for working and setting time. Different letters indicate significant differences between mean values of working and setting times (p < 0.0001).

3.5. Compressive Strength (CS)

Figure 5 depicts the results for compressive strength. The addition of Biosilicate® to Maxxion R (Figure 5A) did not compromise the CS. No significant differences were found between the Maxxion R groups. In contrast, for Fuji IX groups

(Figure 5B), the compressive strength decreased by approximately 30% for F5%, 37% for F10%, and 43% for F15% compared to F0%. ($p < 0.0001$). The F10% group did not differ from the F5% and F15% groups. However, F5% was significantly higher than F15% ($p = 0.0126$). Fuji IX groups exhibited a higher compressive strength than Maxxion R, with a maximum value of 149 MPa compared to 75 MPa for Maxxion R.

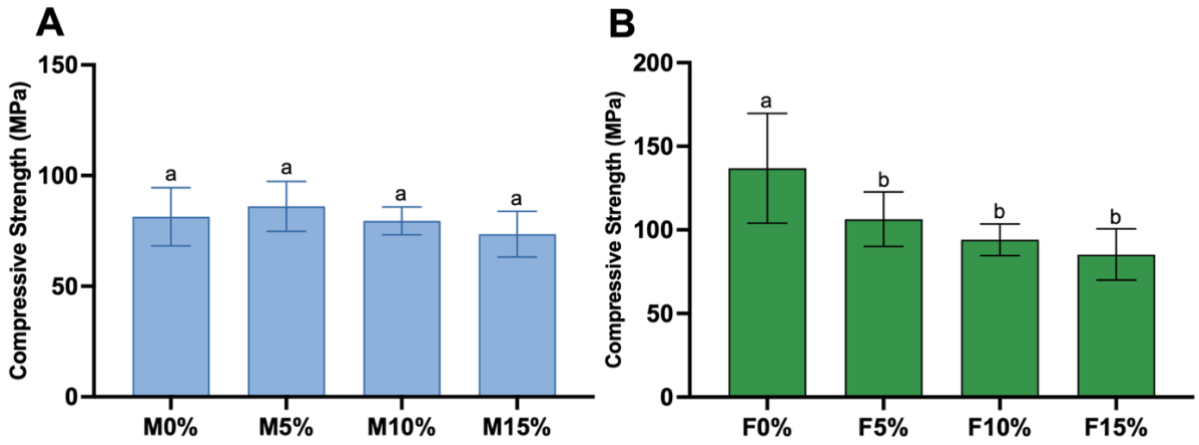

Figure 5. Compressive strengths of GICs. Figure 5A: Maxxion without Biosilicate® ® (M0%), M5%, M10% and M15%. Figure 5B: Fuji XI without Biosilicate® (F0%), F5%, F10% and F15%. Error bars represent standard deviations. Different lowercase letters indicate significant differences among mean values of compressive strength (MPa) in groups ($p<0.0001$).

3.1. Ion release

Figure 6 depicts ions released (ppm) by GICs after 24 h of soaking. In general, for Maxxion R and Fuji IX groups the higher concentration of Biosilicate® was added, the greater amount of the studied ions released, except for Al ion released by Maxxion (3.1.3).

3.1.1 Ca ions

Compared to Fuji IX groups, Maxxion R (Figure 6A) released a greater amount of Ca ions. M15% released the highest amount of calcium (31 ppm), followed by M10% (12 ppm). M5% and M0% did not differ statistically and released approximately 9 ppm of Ca ions. Group F0% exhibited a release of zero ppm of Ca ions. F5% and F10% did not differ significantly and released a small amount of Ca, approximately 0.5 ppm, as shown in Figure 6G. F15% released a significantly higher amount (3 ppm).

3.1.2 Na ions

All Maxxion R groups (Figure 6B) differed significantly from one another: M15% (290 ppm) > M10% (180 ppm) > M5% (120 ppm) > M0% (80 ppm). For Fuji IX (Figure 6H), F15% released a higher amount of 100 ppm, followed by F10% and F5%, which were statistically similar (12 ppm) ($p = 0.2086$). F0% released the lowest amount (3 ppm).

3.1.3 Al ions

M15% released an average of 60 ppm of Al ions, whereas M5%, M0%, and M10% did not differ statistically, releasing approximately 100 ppm. The highest Al release for Fuji IX groups (Figure 6I) was observed for F15% (8 ppm), followed by F10% (2 ppm). F0% and F5% did not differ statistically and presented the lowest Al release.

3.1.4 Si ions

M15% released significantly more Si ions than the other Maxxion R groups (38 ppm; see Figure 6D). M5% and M10% released about 28 ppm, and they were not sgnificantly different ($p = 0.9981$). M0% released the lowest amount fo Si ions (19 ppm). For Fuji IX (Figure 6J), all groups were significantly different from each other ($p < 0.0001$): F15% (25 ppm) > F10% (7 ppm) > F5% (4 ppm) > F0% (1 ppm), with a decreasing amount of Si ions released as the concentration decreased.

3.1.5 P ion

M15% released the most significant amount of P ions (40 ppm), whereas M0% released the lowest amount (11 ppm). M5% and M10% were not statistically different (approximately, 30 ppm) (Figure 6E). No P ions was detected or quantified F0%. The P ion release by F5%, F10%, and F15% was made possible by incorporating Biosilicate®. F5% (0.5 ppm) did not differ statistically from F0% ($p = 0.4751$). F10% (1ppm) was statistically higher than F0% and F5% ($p < 0.0001$). F15% released the highest amount of P ions among Fuji IX groups (9 ppm) (Figure 6K).

3.1.6 F ion

The incorporation of Biosilicate® to Maxxion R increased F ion release by a factor of 4, and by a factor of 2.5 for Fuji IX. M15% released the highest amount of F

ion (40 ppm), followed by M10% and M5% (35 ppm), that did not differ statistically between them. M0% presented a significant lower (5 ppm) F ion release (Figure 6F). Fuji IX by itself (F0%), showed the lowest amount of fluoride release, at 2.5 ppm. F5% released a significant higher amount (5.7 ppm) compared do F0% ($p < 0.0001$). The highest amount was observed for F15% (7 ppm), which not differ statistically ($p = 0.8187$) from F10% (6.3 ppm) as shown in Figure 6L.

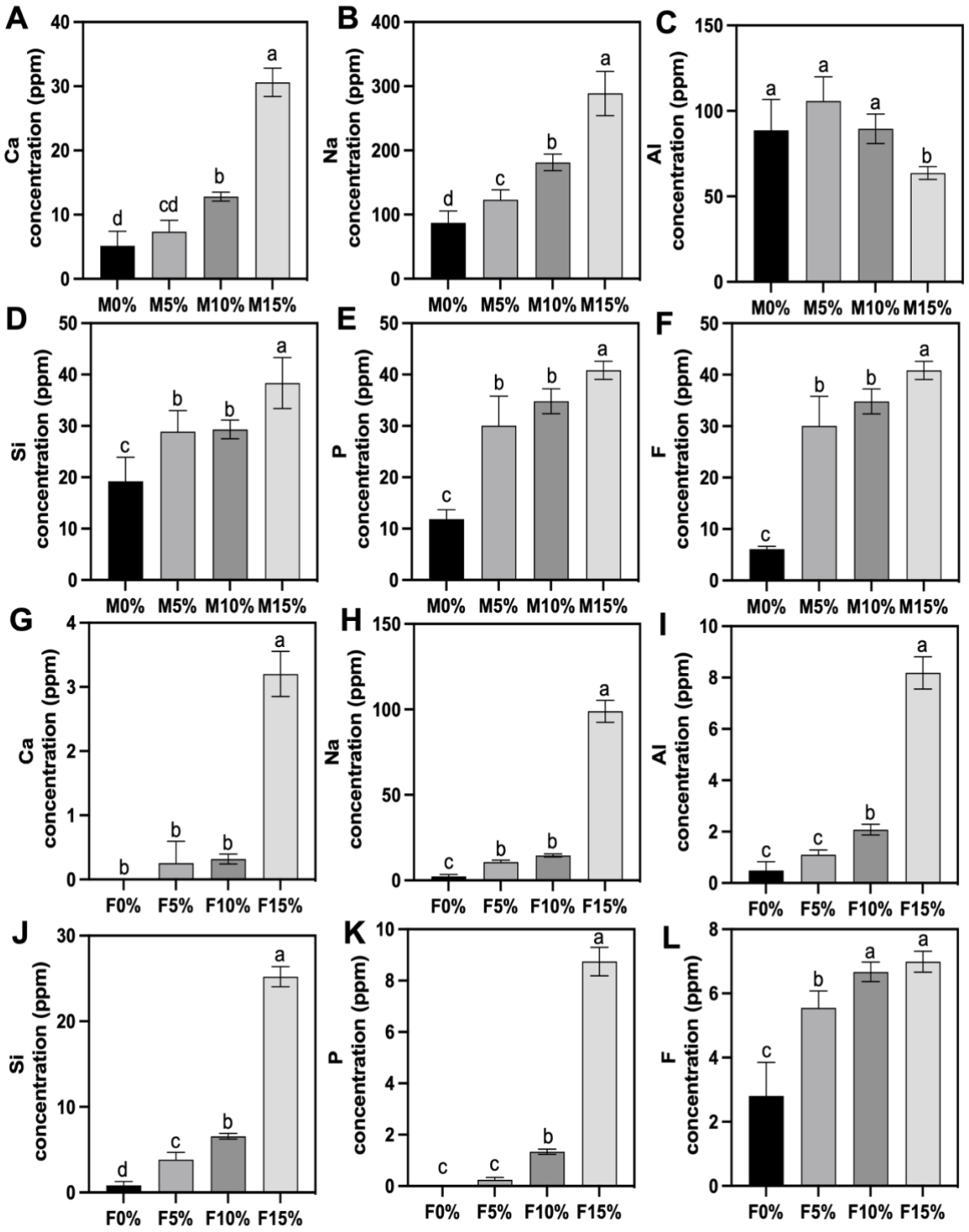

Figure 6. Concentration of ions released in 24 h. Na, Al, Si, P, and Ca determination on the eluates by ICP OES, and F by UV-Vis. Different letters indicate significant differences in the amount (ppm) of the ion released by each group (Maxxion R: Figure 6A-F; Fuji IX: Figure 6G-L).

3.4 Cytotocixity

Figure 7 depicts the percentage of cell death relative to positive control. The percentage of dead cells was calculated relative to lysis buffer (positive control) set to 100%. M5% presented a significantly higher percentage of dead cells compared to M0% ($p < 0.0001$) and M15% ($p < 0.0001$). M5% appears to be the most cytotoxic since it was the only treatment significantly different from the negative control ($p = 0.0009$). The next most cytotoxic group was M10%, which did not differ from M5% ($p > 0.9999$). Among those Maxxion R groups with Biosilicate®, only M15% did not differ from the M0% ($p = 0.0541$). A tendency toward decreased cytotoxicity when concentrations above 5% of Biosilicate® have been incorporated was observed. In the Fuji IX groups (Figure 7B), Biosilicate® incorporation did not have an impact on the material cytotoxicity, as F0%, F5%, F10%, F15%, and CCM groups showed were not significantly different ($p > 0.9999$).

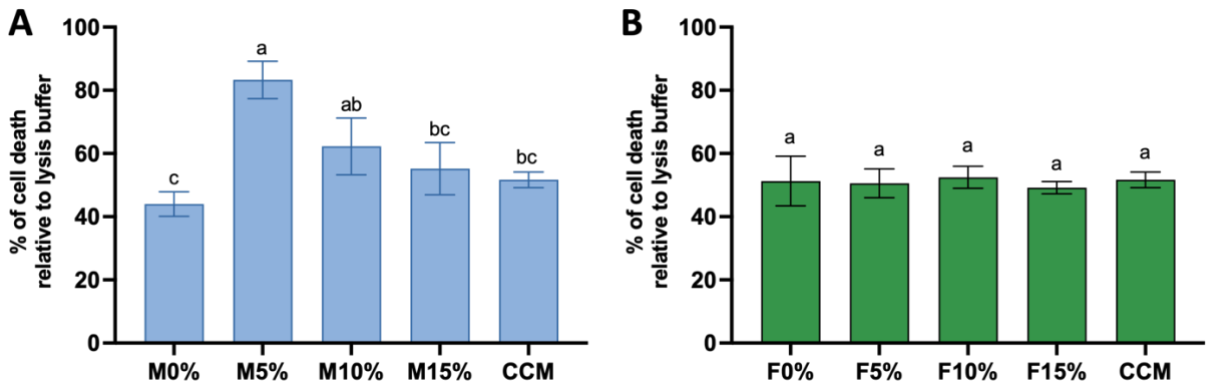

Figure 7. Cytotoxicity at 24 h. Percentage of cell death relative to the lysis buffer (100% of death), while the negative control cells were exposed only to the cell culture medium. Different letter represents statistical differences on the charts.

3.4 Antimicrobial activity

Data were analyzed by Kruskal–Wallis and Dunn's multiple comparisons test. After *S. mutans* specimen exposure a 1-log reduction in surviving bacteria was observed for all Maxxion groups compared to the N group (no specimen, only bacteria). M5% consistently reduced *S. mutans* by 4- to 5-logs compared to all other groups. No colonies (zero) were observed on the plates, meaning less than 100 CFU/mL remained after direct contact with M5% (indicated by the black diamond on Figure 8A). Therefore, statistical analysis was run comparing M0%, M10%, M15%, and N groups. Only M0% ($p = 0.0053$) and M10% ($p = 0.0093$) showed statistically reduced CFU after exposure compared to N group, although, there was no significant difference among M0%,

M10%, and M15%. No significant reduction in CFU was found for all Fuji IX groups when compared to each other nor when compared to N group (Figure 8B).

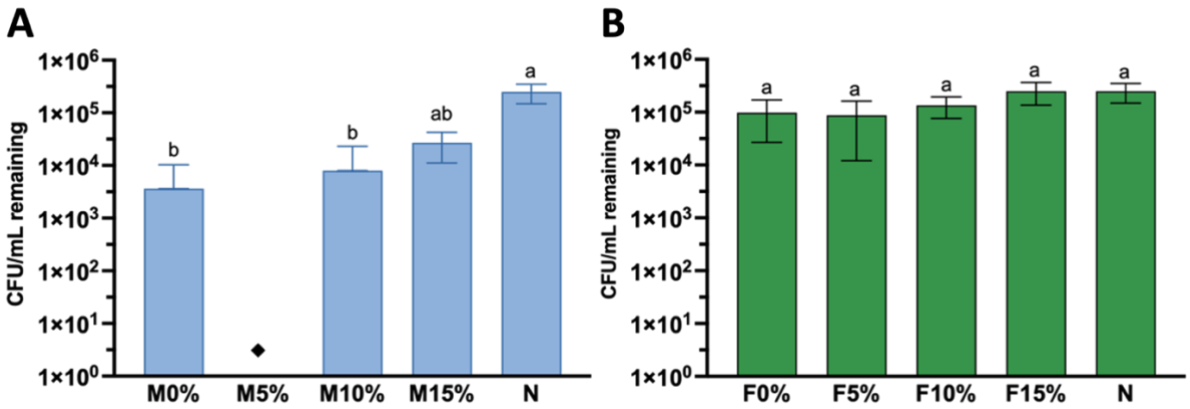

Figure 8. *S. mutans* remaining after 2 h of direct contact with Maxxion groups (8A) and Fuji groups (8B). Black diamond (◆) indicates less than 100 CFU/mL recovered (limit of detection). Different letters indicate significant differences among groups ($p < 0.0001$).

The percentage of survival of *S. mutans* after 2 h of direct contact was calculated using N group as 100% of survival as reference. Overall, Maxxion R and Fuji IX groups showed substantial differences in overall *S. mutans* survival. As shown in Figure 9A, M5% presented 0% (± 0.0) of survival rate, followed by M0% at 1.2% (± 2.7), M10% at 4.7% (± 0.8), and M15% at 12.5% (± 5.3). M5% consistently differ from M15% ($p = 0.0046$). Regarding Fuji IX groups (Figure 9B), no significant differences were observed on survival rate for F0%, F5%, F10%, and F15% ($p > 0.0001$). Fuji 5% trended towards being the most effective in antimicrobial effect among Fuji IX groups, presenting 29.4% (± 10.7) of survival compared to no specimen. F0% and F10% presented an intermediate percentage of survival, respectively 29.4 (± 14.9) and 60.9 (± 5.3). F15% increased *S. mutans* survival in 8.1% (± 5.9), but none of these differences reached statistical significance.

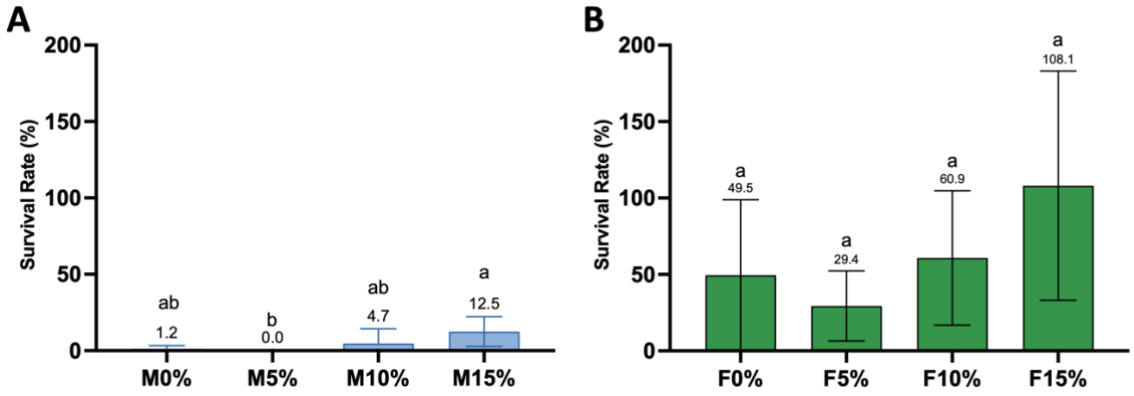

Figure 9. Percentage of survival of *S. mutans* compared to no disk group (only bacteria) for Maxxion groups (figure 9A) and Fuji groups (figure 9B). No disk was considered 100% survival. Different letters indicate significant differences among groups.

4. Discussion

The purpose of this exploratory study was to assess the impact of incorporating different concentrations of bioactive glass ceramic (Biosilicate® 23,75Na_2O–23,75CaO–48,5SiO_2–4P_2O_5) into a conventional (Maxxion R) and a high viscosity (Fuji IX) glass ionomer cement. The first research hypothesis was accepted because the addition of Biosilicate® into GICs affected their setting times and mechanical behavior. For conventional GIC (Maxxion R), only M5% demonstrated comparable setting/working times to M0%. However, adding 10% Biosilicate® to Maxxion resulted in a significant increase in setting time, whereas adding 15% Biosilicate® resulted in shorter setting times. However, previous studies showed that the amount of bioglass or ceramic powders added to GIC increases proportionally their setting time [17,18] which was the opposite observed in M15% setting behavior. For the GIC with a high viscosity (Fuji IX), all experimental groups demonstrated significantly increased working/setting times. In addition, no significant differences in compressive strength (CS) were observed between Maxxion R groups; however, CS of the experimental Fuji IX cements decreased.

Comparing the obtained peaks to the setting mechanism of conventional glass ionomer cement, as reported by other authors, the FTIR spectrum revealed very minor structural changes [32,38,39]. What stands out in the FTIR spectrum is the constant formation of polysalts and the inversional behavior of polyacrylic acid (–COOH) with time, indicating that there is an interaction between the Biosilicate® and GIC. The polycarboxylate salts in the range of 1400 to 1640 cm^{-1} [31] were also observed in the

present study (clearly indicated between dashed lines in Figure 3. This range is associated to calcium carboxylate (–$COOCa^{2+}$) at 1409 cm^{-1}, aluminum carboxylate (–$COOAl^{3+}$) at 1459 cm^{-1}, and sodium carboxylate (–$COONa^{2+}$) at 1552 cm^{-1} [29,30,32].

It must be considered that, due to the use of different GICs with different powder and liquid phase compositions, different behaviors on the analyzed properties are to be anticipated. Fuji IX's powder contains fluoroaluminosilicate glass particles and lyophilized PAA, meaning that water must first dissolve PAA in the powder in order to initiate an acid/base reaction. Maxxion's powder contains fluoroaluminosilicate and calcium fluoride, and the liquid contains polycarboxylic acid, tartaric acid, and water. Concerning Fuji experimental groups, the presence of Biosilicate may have hindered the hydration of polyacrylic acid (PAA), reducing PAA ionization and, as a result, reducing the leaching of cationic ions by the acid attack on the glass, reducing the formation of crosslinks in the matrix, and also increasing the working time.

Additionally, the P/L ratio was altered from 3.6/1 to 1.8/1 (wt/wt) to improve handling conditions. It is well-known that the P/L ratio, the concentration of the polyacid, and the particle size of the powder influence not only the working and setting times, but also the mechanical properties. [14,44]. In this sense, the addition of Biosilicate® did not affect the compressive strength of Maxxion groups because the P/L ratio remained unaltered. However, for Fuji IX experimental groups (F5%, F10%, and F15%) the P/L ratio seems to be critical for CS. Thus, a decrease in CS for these groups were expected.

In addition to differences in the powder compositions of Maxxion R and Fuji IX, it is important to mention that the brand-specific polyacid type can influence the physico-mechanical properties of the GICs [40]. The polyacids used in conventional glass ionomers, such as Maxxion R, are less concentrated and less viscous than those used in high viscosity GICs, such as Fuji IX [7,41]. The concentration and molecular weight of polycarboxylic acid have a significant effect on mechanical properties [12,41]. This may explain why Fuji XI exhibited superior overall mechanical properties compared to Maxxion R (Figure 6).

It has been reported that certain formulation of bioglass containing Al^{3+} increased the CS of GICs in comparison to formulation without Al^{3+} [42]. In addition, sodium-containing bioglasses showed a degrading effect on GICs, whereas sodium-free formulations did not compromise setting or mechanical properties [17,19,43]. Biosilicate® contains sodium oxide (23.75% by wt), and no aluminum. Following the

partial replacement of GIC powder with bioactive glass ceramic, the amount of aluminum cations (Al^{3+}) was reduced. Al^{3+} is a major contributor to strength because it forms three-dimensional and stronger bonds than Ca^{2+} in the GIC matrix [44]. Any imbalance in this process or interference with the glass degradation can influence the cement's setting and, consequently, its mechanical properties. [45].

Certain bioactive glasses with a high sodium content can release Na^{+} during the acid-base reaction, interfering with the cement setting reaction, negatively impacting mechanical properties, and extending the setting time [4,42]. In addition, the Al:Si ratio of approximately 1:2 in glass is essential for a satisfactory setting reaction rate, hydrolytic stability, and the ability of glass to form cements [46-48]. It is also possible that an unbalanced Al:Si ratio occurred in those cements, which was not directly measured in this study after the Biosilicate® was incorporated by %wt.

According to ISO 9917-1:2007, this material must have a minimum working time of 1.5 minutes and a maximum setting time of 6 minutes. Only F0% demonstrated setting time in accordance with ISO 9917, indicating that M0% falls short of the specifications. In addition, only F0% and F5% exhibited CS values greater than 100 MPa as required by ISO 9917-1:2007, whereas Maxxion groups fell below the requirement, indicating that adjustments must be made to those experimental cements. For improved setting behaviors and mechanical properties, it would be beneficial to test the reaction of various polyacids with bioglass or bioglass ceramic containing GIC. In conventional GIC, the initial setting reaction involves the neutralization between the aqueous polyacid and the glass powder. [5]. This reaction forms calcium (or strontium) polyacrylate immediately, with aluminium polyacrylate forming slightly later [6].

As Biosilicate® is a rich in Ca and Na, the abundance of these ions bound to the polymer chains may induce charge repulsions, thereby reducing Al^{3+} binding [12,43], thereby affecting setting behaviors and mechanical properties. The potential primary reason is that polyacrylic acid (PAA) has only one carboxyl group per repeating unit [49,50], whereas Poly (vinylphosphonic-co-acrylic acid) which is used as a rate-modifier in a few commercial brands [13], has a phosphonic acid group in addition to the carboxyl group. This allows more protons to attack the glass, but also promotes the formation of more ionic cross-links between metallic cations such as Al^{3+} and the polymeric acid, thereby enhancing the hydrolytic stability and mechanical properties of cements [38].

All experimental groups presented crack lines, unreacted particles, and rough surfaces. Small particle clusters of Biosilicate® were also observed in the experimental cements. These concerns are commonly observed for bioglass-containing GICs [20]. Still, Fuji IX groups exhibited the smoothest surface, fewer pores, and fewer crack lines than Maxxion R groups. It may be due to differences in the composition, particle size, and P/L ratio of these GICs [51,52]. Lower concentrations (F5% and M5%) of the bioactive glass ceramic induced fewer microstructural disturbances in the GICs.

Higher Biosilicate® concentrations resulted in greater ion release from GICs, thus supporting the acceptance of the second research hypothesis. Overall, the release of Na, Si, P, and F increased with increasing Biosilicate® concentration. However, for Ca ion releasing, only F15% for Fuji IX and M10% and M15% for Maxxion R were significantly higher. Also, Al release was significant lower in M15%, indicating that somehow Biosilicate® in this concentration decreased Al release. The profile of ion release in descending order for Maxxion R groups was Na>Al>Si=P=F>Ca, and for Fuji IX was Na>Si>Al=P=F>Ca. Figure 6 clearly depicts that Maxxion R groups released a greater quantity of all evaluated ions than Fuji IX groups.

One of the most notable variations was the range of Al released by Maxxion R groups (60 to 105 ppm) versus Fuji IX groups (< 1 to 8 ppm), which can be attributed to the different compositions of the two cements (i.e., Maxxion R presents Ca_2F and NaF in its composition, while Fuji IX does not). It has been reported that larger cations, such as Ca and Na, disrupt the glass network more effectively, resulting in a decrease in oxygen density (expanded glass network) and allowing a greater amount of small cations (e.g., Al) to diffuse through the glass. Thus, it is hypothesized that the Al in Fuji powder was crosslinked via carboxylate salts and entrapped within the GIC matrix, resulting in a low Al release once the Biosilicate®-derived Ca is available to react and is released.

As mentioned previously, the release of fluoride ions is one of the primary benefits of using GICs [7,8]. Fluoride increases the acid resistance of teeth by inhibiting demineralization and enhancing remineralization, and it inhibits the growth and metabolism of bacteria by inhibiting the activities of enzymes such as enolase and ATPase. [10,11]. In this regard, the addition of Biosilicate® increased the fluoride release by a factor of 4 for Maxxion R and 2.5 for Fuji IX (Figures 6F and 6L). Therapeutic ion release increased proportionally with Biosilicate® addition for both

GICs, suggesting that these materials may be effective for remineralizing enamel and dentin.

The third research hypothesis, that Biosilicate® improves biocompatibility, was disproved as we observed no difference in cytotoxicity among the Fuji IX groups, while the rate of cell death in M5% and M10% was significantly higher than in M0%. For Fuji IX, this can be partially attributed to the high alkalinity of Biosilicate®, which indicates that the glass ceramic likely compensates the acidity in those groups with a 1.8/1 ratio (g/g), making them similar to F0% [ratio 3.6/1 (wt/wt)]. The low amount of ions, particularly Al ions, released by Fuji IX groups may also be a factor in the lack of cytotoxicity.

In contrast, the amount of realeased ions, primarily Al and Na, was substantial in the Maxxion R groups. M5%, which released 105 ppm of Al, tends to exhibit the most cytotoxic effect. It has been demonstrated that as Al concentration increases (4.5 ppm, 45 ppm, and 450 ppm), the percentage of live cells in a population decreases, while the percentage of early apoptotic cells, late apoptotic cells, and dead cells increases [53]. The primary mechanism of Al toxicity is the induction of oxidative stress by excessive production of reactive oxygen species (ROS) [54], which disrupts signaling processes, inhibits cell growth, promotes DNA damage [55,56], destroys phospholipidic membranes, and induces cellular apoptosis [57].

The fourth research hypothesis that the higher the amount of Biosilicate® added to GIC, the greater the inhibition of *S. mutans*, was also rejected. Figure 4A clearly demonstrates that only M5% consistently killed *S. mutans* to levels below our limit of detection (less than 100 CFU/ml). M0% and M10% also significantly killed *S. mutans* compared to the No Disk control (N), but this killing was not significantly different than that of M15%. As previously stated, a greater amount of Al was released by M5% (105 ppm), and so there is likely a higher amount of Al free in the M5% surfaces which may have contributed to the antimicrobial killing measured by the direct contact assay.

It is well known that Al can act synergistically with fluoride increasing the bactericidal effect on *S. mutans* by inhibiting ATPase [58]. The possible mechanism of the combined action of fluoride and aluminum to inhibit ATPase may involve the formation of an ADP-Al-F_3 complex in the enzyme's catalytic site [59,60]. ATPase plays an important role in the maintenance of the intracellular pH by pumping out protons; inhibition of this enzyme disrupts the bacterial metabolism and the aciduric capability of *S. mutans* [61].

A significant reduction in *S. mutans (*NCTC 10449) growth after exposure to F^-, Al^{3+}, and SiO_3^{2-}, at respective concentrations 8.6 ppm, 6.8 ppm, and 9.7 ppm has been reported previously [63]. It has been reported a significant reduction in *S.mutans (*NCTC10449) growth after exposure to F^-, Al^{3+}, and SiO_3^{2-}, at respective concentrations 8.6 pp , 6.8 ppm, and 9.7 ppm [63]. In the same study, it was demonstrated that as the concentration of all ions increased, the inhibitory effect tended to increase. In this study M5% released 30 ppm of F^-, 105 ppm of Al^{3+}, and 19 ppm of SiO_3^{2-}. It is possible that the combination of these ions promoted increased bactericidal activity against *S. mutans*, with Al being the primary contributor to the antimicrobial effect observed on the surface of M5%, and F and Si being minor contributors.

Lastly, this was a prospection and comprehension study designed to better comprehend the potential benefits of the interaction between Biosilicate® and two distinct GICs. In this study, the manufacturer-provided composition and the lack of information regarding the amount of each element in the matrix were insufficient to comprehend the interaction between the studied elements. This lack of compositional information required a surface analysis via energy-dispersive X-ray spectroscopy (EDS).

Despite the encouraging developments presented in this article for the enhancement of the ion-releasing and antimicrobial effects of GICs, additional studies employing various glass ceramic compositions are required to investigate this topic in greater depth. For instance, by increasing the amount of aluminum and decreasing the amount of calcium and sodium; by adding uniformly smaller Biosilicate®; and by employing different methods for incorporating glass ceramic into GIC (such as molar ratio instead of %wt, including automated methods for better homogenization of powders and different formulations of polyacid with co-polymers in place of PAA.

5.Conclusion

The bioactive glass ceramic Biosilicate® used in this study did not significantly affect the setting and mechanical properties of Maxxion R when incorporated at a 5% (%wt), and it provided benefits such as therapeutic ion release and antimicrobial activity. Fuji IX's cytotoxicity was unchanged with the addition of Biosilicate®, and the release of therapeutic (Si, P, Na, and Ca) ions was increased. However, Fuji IX's

setting behavior was altered, and its mechanical properties were diminished, due to changes in P/L ratio and Biosilicate® addition.

Author Contributions: Conceptualization, E.D.Z, G.A.P.M, M.T.S, and R.M.PR; methodology, G.A.P.M., J.T., C.S., L.Y., A.O.M. , M.T.S, R.R.P and R.M.P.R; software, G.A.P.M, MTS, J.T, C.S and R.R.P; formal analysis, G.A.P.M, MTS, J.T, C.S and R.R.P, R.M.P.R; investigation, G.A.P.M, M.T.S, J.T, C.S, R.R.P and R.M.PR; resources E.D.Z, M.T.S, and RRP; data curation, G.A.P.M., J.T., C.S., L.Y., M.T.S, and R.R.P., R.M.P.R; writing, original draft preparation, G.A.P.M; writing, review and editing, R.M.PR, R.R.P, J.T, C.S, and M.T.S; supervision, RMPR; project administration, G.A.P.M. and R.M.PR. All authors have read and agreed to the published version of the manuscript.

Funding: This research was funded by National Council for Scientific and Technological Development (CNPq), grant number 141450/2020-7. This research was also partially supported by the University of Detroit Mercy School of Dentistry.

Acknowledgments: The authors would like to thank the Center for Research, Education and Technology in Vitreous Materials (CeRTEV), Federal University of São Carlos (UFSCAR) that kindly provided the glass ceramic, Biosilicate®. The University of Detroit Mercy School of Dentistry. The National Council for Scientific and Technological Development (CNPq) Process 141450/2020-7.

Conflicts of Interest: The authors of this study have no conflicts of interest to disclose, and do not have any financial interest in the companies whose materials are included in this article. The funders had no role in the design of the study; in the collection, analyses, or interpretation of data; in the writing of the manuscript, or in the decision to publish the results.

References

1. Frencken, J.E. The ART approach using glass-ionomers in relation to global oral health care. *Dent Mater* **2010**, *26*, 1-6, doi:10.1016/j.dental.2009.08.013.
2. Frencken, J.E.; Pilot, T.; Songpaisan, Y.; Phantumvanit, P. Atraumatic restorative treatment (ART): rationale, technique, and development. *J Public Health Dent* **1996**, *56*, 135-140; discussion 161-133, doi:10.1111/j.1752-7325.1996.tb02423.x.
3. Frencken, J.E.; Leal, S.C.; Navarro, M.F. Twenty-five-year atraumatic restorative treatment (ART) approach: a comprehensive overview. *Clin Oral Investig* **2012**, *16*, 1337-1346, doi:10.1007/s00784-012-0783-4.
4. Hill, R. Glass ionomer polyalkenoate cements and related materials: past, present and future. *Br Dent J* **2022**, *232*, 653-657, doi:10.1038/s41415-022-4239-1.
5. Sidhu, S.K.; Nicholson, J.W. A Review of Glass-Ionomer Cements for Clinical Dentistry. *J Funct Biomater* **2016**, *7*, doi:10.3390/jfb7030016.
6. Nicholson, J.W.; Brookman, P.J.; Lacy, O.M.; Wilson, A.D. Fourier transform infrared spectroscopic study of the role of tartaric acid in glass-ionomer dental cements. *J Dent Res* **1988**, *67*, 1451-1454, doi:10.1177/00220345880670120201.
7. Nicholson, J.W. Maturation processes in glass-ionomer dental cements. *Acta Biomater Odontol Scand* **2018**, *4*, 63-71, doi:10.1080/23337931.2018.1497492.
8. Komatsu, H.; Shimokobe, H.; Kawakami, S.; Yoshimura, M. Caries-preventive effect of glass ionomer sealant reapplication: study presents three-year results. *J Am Dent Assoc* **1994**, *125*, 543-549, doi:10.14219/jada.archive.1994.0082.
9. Liao, Y.; Brandt, B.W.; Li, J.; Crielaard, W.; Van Loveren, C.; Deng, D.M. Fluoride resistance in Streptococcus mutans: a mini review. *J Oral Microbiol* **2017**, *9*, 1344509, doi:10.1080/20002297.2017.1344509.
10. Oh, H.J.; Oh, H.W.; Lee, D.W.; Kim, C.H.; Ahn, J.Y.; Kim, Y.; Shin, H.B.; Kim, C.Y.; Park, S.H.; Jeon, J.G. Chronologic Trends in Studies on Fluoride Mechanisms of Action. *J Dent Res* **2017**, *96*, 1353-1360, doi:10.1177/0022034517717680.
11. Ten Cate, J.M. Fluorides in caries prevention and control: empiricism or science. *Caries Res* **2004**, *38*, 254-257, doi:10.1159/000077763.

12. Alhalawani, A.M.; Curran, D.J.; Boyd, D.; Towler, M.R. The role of poly (acrylic acid) in conventional glass polyalkenoate cements. *Journal of Polymer Engineering* **2016**, *36*, 221-237.
13. Nicholson, J. Glass-ionomer cements for clinical dentistry. *Mater. Technol* **2010**, *25*, 8-13.
14. Binaljadm, T.; Moorehead, R.; Almela, T.; Franklin, K.; Tayebi, L.; Moharamzadeh, K. Biomodification of a Class-V Restorative Material by Incorporation of Bioactive Agents. *Dent J (Basel)* **2019**, *7*, doi:10.3390/dj7040110.
15. Autefage, H.; Gentleman, E.; Littmann, E.; Hedegaard, M.A.; Von Erlach, T.; O'Donnell, M.; Burden, F.R.; Winkler, D.A.; Stevens, M.M. Sparse feature selection methods identify unexpected global cellular response to strontium-containing materials. *Proc Natl Acad Sci U S A* **2015**, *112*, 4280-4285, doi:10.1073/pnas.1419799112.
16. Gentleman, E.; Fredholm, Y.C.; Jell, G.; Lotfibakhshaiesh, N.; O'Donnell, M.D.; Hill, R.G.; Stevens, M.M. The effects of strontium-substituted bioactive glasses on osteoblasts and osteoclasts in vitro. *Biomaterials* **2010**, *31*, 3949-3956, doi:10.1016/j.biomaterials.2010.01.121.
17. Choi, J.Y.; Lee, H.H.; Kim, H.W. Bioactive sol-gel glass added ionomer cement for the regeneration of tooth structure. *J Mater Sci Mater Med* **2008**, *19*, 3287-3294, doi:10.1007/s10856-008-3464-8.
18. Kim, D.A.; Lee, J.H.; Jun, S.K.; Kim, H.W.; Eltohamy, M.; Lee, H.H. Sol-gel-derived bioactive glass nanoparticle-incorporated glass ionomer cement with or without chitosan for enhanced mechanical and biomineralization properties. *Dent Mater* **2017**, *33*, 805-817, doi:10.1016/j.dental.2017.04.017.
19. Kim, H.J.; Bae, H.E.; Lee, J.E.; Park, I.S.; Kim, H.G.; Kwon, J.; Kim, D.S. Effects of bioactive glass incorporation into glass ionomer cement on demineralized dentin. *Sci Rep* **2021**, *11*, 7016, doi:10.1038/s41598-021-86481-y.
20. Yli-Urpo, H.; Lassila, L.V.; Närhi, T.; Vallittu, P.K. Compressive strength and surface characterization of glass ionomer cements modified by particles of bioactive glass. *Dent Mater* **2005**, *21*, 201-209, doi:10.1016/j.dental.2004.03.006.
21. Jones, J.R. Review of bioactive glass: from Hench to hybrids. *Acta Biomater* **2013**, *9*, 4457-4486, doi:10.1016/j.actbio.2012.08.023.

22. Black, J.; Hastings, G. *Handbook of biomaterial properties*; Springer Science & Business Media: 2013.
23. Crovace, M.C.; Souza, M.T.; Chinaglia, C.R.; Peitl, O.; Zanotto, E.D. Biosilicate®—A multipurpose, highly bioactive glass-ceramic. In vitro, in vivo and clinical trials. *Journal of Non-Crystalline Solids* **2016**, *432*, 90-110.
24. Peitl, O.; Zanotto, E.D.; Serbena, F.C.; Hench, L.L. Compositional and microstructural design of highly bioactive P2O5-Na2O-CaO-SiO2 glass-ceramics. *Acta Biomater* **2012**, *8*, 321-332, doi:10.1016/j.actbio.2011.10.014.
25. Tirapelli, C.; Panzeri, H.; Lara, E.H.; Soares, R.G.; Peitl, O.; Zanotto, E.D. The effect of a novel crystallised bioactive glass-ceramic powder on dentine hypersensitivity: a long-term clinical study. *J Oral Rehabil* **2011**, *38*, 253-262, doi:10.1111/j.1365-2842.2010.02157.x.
26. Rastelli, A.; Nicolodelli, G.; Romano, R.; Milori, D.; Perazzoli, I.; Ferreira, E.; Pedroso, A.; Souza, M.; Peitl, O.; Zanotto, E. After bleaching enamel remineralization using a bioactive glass-ceramic (BioSilicate®). *Biomedical glasses* **2016**, *2*.
27. de Araújo Lopes, J.M.; Benetti, F.; Rezende, G.C.; Souza, M.T.; Conti, L.C.; Ervolino, E.; Jacinto, R.C.; Zanotto, E.D.; Cintra, L.T.A. Biocompatibility, induction of mineralization and antimicrobial activity of experimental intracanal pastes based on glass and glass-ceramic materials. *Int Endod J* **2020**, *53*, 1494-1505, doi:10.1111/iej.13382.
28. Pacheco, R.R.; Garcia-Flores, A.F.; Soto-Montero, J.R.; Lesseux, G.G.; Lancelotti, A.; Martinez, E.D.; Rettori, C.; Urbano, R.R.; Rueggeberg, F.A.; Giannini, M. Synthesis, characterization, and incorporation of upconverting nanoparticles into a dental adhesive. *Braz Oral Res* **2021**, *35*, e120, doi:10.1590/1807-3107bor-2021.vol35.0120.
29. Tsuzuki, F.M.; Pascotto, R.C.; Malacarne, L.C.; Bento, A.C.; Medina Neto, A.; de Castro-Hoshino, L.V.; Souza, M.; Nicholson, J.W.; Baesso, M.L. Studies of the early stages of the dynamic setting process of chemically activated restorative glass-ionomer cements. *Biomater Investig Dent* **2021**, *8*, 39-47, doi:10.1080/26415275.2021.1898964.
30. Panpisut, P.; Monmaturapoj, N.; Srion, A.; Toneluck, A.; Phantumvanit, P. Physical Properties of Glass Ionomer Cement Containing Pre-Reacted

Spherical Glass Fillers. *Braz Dent J* **2020**, *31*, 445-452, doi:10.1590/0103-6440202003276.

31. Talal, A.; Tanner, K.E.; Billington, R.; Pearson, G.J. Effect of ultrasound on the setting characteristics of glass ionomer cements studied by Fourier transform infrared spectroscopy. *J Mater Sci Mater Med* **2009**, *20*, 405-411, doi:10.1007/s10856-008-3578-z.
32. Yamakami, S.A.; Ubaldini, A.L.M.; Sato, F.; Medina Neto, A.; Pascotto, R.C.; Baesso, M.L. Study of the chemical interaction between a high-viscosity glass ionomer cement and dentin. *J Appl Oral Sci* **2018**, *26*, e20170384, doi:10.1590/1678-7757-2017-0384.
33. Chen, S.; Cai, Y.; Engqvist, H.; Xia, W. Enhanced bioactivity of glass ionomer cement by incorporating calcium silicates. *Biomatter* **2016**, *6*, e1123842, doi:10.1080/21592535.2015.1123842.
34. Gandolfi, M.G.; Taddei, P.; Siboni, F.; Modena, E.; Ciapetti, G.; Prati, C. Development of the foremost light-curable calcium-silicate MTA cement as root-end in oral surgery. Chemical-physical properties, bioactivity and biological behavior. *Dent Mater* **2011**, *27*, e134-157, doi:10.1016/j.dental.2011.03.011.
35. Nicholson, J.W.; Coleman, N.J.; Sidhu, S.K. Kinetics of ion release from a conventional glass-ionomer cement. *J Mater Sci Mater Med* **2021**, *32*, 30, doi:10.1007/s10856-021-06501-1.
36. Kunert, M.; Rozpedek-Kaminska, W.; Galita, G.; Sauro, S.; Bourgi, R.; Hardan, L.; Majsterek, I.; Lukomska-Szymanska, M. The Cytotoxicity and Genotoxicity of Bioactive Dental Materials. *Cells* **2022**, *11*, doi:10.3390/cells11203238.
37. Pinto, T.S.; Lima, O.A.d.; Leal Filho, L.d.S. Sphericity of apatite particles determined by gas permeability through packed beds. *Mining, Metallurgy & Exploration* **2009**, *26*, 105-108.
38. Fuchs, M.; Gentleman, E.; Shahid, S.; Hill, R.G.; Brauer, D.S. Therapeutic ion-releasing bioactive glass ionomer cements with improved mechanical strength and radiopacity. *Frontiers in Materials* **2015**, 63.
39. Matsuya, S.; Matsuya, Y.; Ohta, M. Structure of bioactive glass and its application to glass ionomer cement. *Dent Mater J* **1999**, *18*, 155-166, doi:10.4012/dmj.18.155.
40. Berg, M.C.; Benetti, A.R.; Telling, M.T.F.; Seydel, T.; Yu, D.; Daemen, L.L.; Bordallo, H.N. Nanoscale Mobility of Aqueous Polyacrylic Acid in Dental

Restorative Cements. *ACS Appl Mater Interfaces* **2018**, *10*, 9904-9915, doi:10.1021/acsami.7b15735.

41. Wilson, A.D.; Hill, R.G.; Warrens, C.P.; Lewis, B.G. The influence of polyacid molecular weight on some properties of glass-ionomer cements. *J Dent Res* **1989**, *68*, 89-94, doi:10.1177/00220345890680021401.
42. De Caluwé, T.; Vercruysse, C.W.; Ladik, I.; Convents, R.; Declercq, H.; Martens, L.C.; Verbeeck, R.M. Addition of bioactive glass to glass ionomer cements: Effect on the physico-chemical properties and biocompatibility. *Dent Mater* **2017**, *33*, e186-e203, doi:10.1016/j.dental.2017.01.007.
43. De Barra, E.; Hill, R.G. Influence of alkali metal ions on the fracture properties of glass polyalkenoate (ionomer) cements. *Biomaterials* **1998**, *19*, 495-502, doi:10.1016/s0142-9612(97)00129-4.
44. Nicholson, J.W.; Czarnecka, B. Review paper: Role of aluminum in glass-ionomer dental cements and its biological effects. *J Biomater Appl* **2009**, *24*, 293-308, doi:10.1177/0885328209344441.
45. Matsuya, S.; Maeda, T.; Ohta, M. IR and NMR analyses of hardening and maturation of glass-ionomer cement. *J Dent Res* **1996**, *75*, 1920-1927, doi:10.1177/00220345960750120201.
46. Kent, B.E.; Lewis, B.G.; Wilson, A.D. Glass ionomer cement formulations: I. The preparation of novel fluoroaluminosilicate glasses high in fluorine. *J Dent Res* **1979**, *58*, 1607-1619, doi:10.1177/00220345790580061001.
47. Moshaverinia, A.; Roohpour, N.; Chee, W.W.; Schricker, S.R. A review of powder modifications in conventional glass-ionomer dental cements. *Journal of materials chemistry* **2011**, *21*, 1319-1328.
48. Wilson, A.D.; Crisp, S.; Prosser, H.J.; Lewis, B.G.; Merson, S.A. Aluminosilicate glasses for polyelectrolyte cements. *Industrial & engineering chemistry product research and development* **1980**, *19*, 263-270.
49. Brauer, D.S.; Gentleman, E.; Farrar, D.F.; Stevens, M.M.; Hill, R.G. Benefits and drawbacks of zinc in glass ionomer bone cements. *Biomed Mater* **2011**, *6*, 045007, doi:10.1088/1748-6041/6/4/045007.
50. Brauer, D.S.; Karpukhina, N.; Kedia, G.; Bhat, A.; Law, R.V.; Radecka, I.; Hill, R.G. Bactericidal strontium-releasing injectable bone cements based on bioactive glasses. *J R Soc Interface* **2013**, *10*, 20120647, doi:10.1098/rsif.2012.0647.

51. Al-Taee, L.; Deb, S.; Banerjee, A. An in vitro assessment of the physical properties of manually- mixed and encapsulated glass-ionomer cements. *BDJ Open* **2020**, *6*, 12, doi:10.1038/s41405-020-0040-x.
52. Behr, M.; Rosentritt, M.; Loher, H.; Handel, G. Effect of variations from the recommended powder/liquid ratio on some properties of resin-modified cements. *Acta Odontol Scand* **2006**, *64*, 214-220, doi:10.1080/00016350600555859.
53. Feng, R.; Chen, L.; Chen, K. Cytotoxicity and changes in gene expression under aluminium potassium sulfate on Spodoptera frugiperda 9 cells. *Ecotoxicology* **2021**, *30*, 2056-2070, doi:10.1007/s10646-021-02478-3.
54. Kumar, V.; Bal, A.; Gill, K.D. Susceptibility of mitochondrial superoxide dismutase to aluminium induced oxidative damage. *Toxicology* **2009**, *255*, 117-123, doi:10.1016/j.tox.2008.10.009.
55. Santos, E.M.; Ball, J.S.; Williams, T.D.; Wu, H.; Ortega, F.; van Aerle, R.; Katsiadaki, I.; Falciani, F.; Viant, M.R.; Chipman, J.K.; et al. Identifying health impacts of exposure to copper using transcriptomics and metabolomics in a fish model. *Environ Sci Technol* **2010**, *44*, 820-826, doi:10.1021/es902558k.
56. Sharma, S.S.; Dietz, K.J. The relationship between metal toxicity and cellular redox imbalance. *Trends Plant Sci* **2009**, *14*, 43-50, doi:10.1016/j.tplants.2008.10.007.
57. Yu, L.; Wu, J.; Zhai, Q.; Tian, F.; Zhao, J.; Zhang, H.; Chen, W. Metabolomic analysis reveals the mechanism of aluminum cytotoxicity in HT-29 cells. *PeerJ* **2019**, *7*, e7524, doi:10.7717/peerj.7524.
58. Sturr, M.G.; Marquis, R.E. Inhibition of proton-translocating ATPases of Streptococcus mutans and Lactobacillus casei by fluoride and aluminum. *Arch Microbiol* **1990**, *155*, 22-27, doi:10.1007/bf00291269.
59. Hayacibara, M.F.; Rosa, O.P.; Koo, H.; Torres, S.A.; Costa, B.; Cury, J.A. Effects of fluoride and aluminum from ionomeric materials on S. mutans biofilm. *J Dent Res* **2003**, *82*, 267-271, doi:10.1177/154405910308200405.
60. Lunardi, J.; Dupuis, A.; Garin, J.; Issartel, J.P.; Michel, L.; Chabre, M.; Vignais, P.V. Inhibition of H+-transporting ATPase by formation of a tight nucleoside diphosphate-fluoroaluminate complex at the catalytic site. *Proc Natl Acad Sci U S A* **1988**, *85*, 8958-8962, doi:10.1073/pnas.85.23.8958.

61. Lemos, J.A.; Palmer, S.R.; Zeng, L.; Wen, Z.T.; Kajfasz, J.K.; Freires, I.A.; Abranches, J.; Brady, L.J. The Biology of Streptococcus mutans. *Microbiol Spectr* **2019**, *7*, doi:10.1128/microbiolspec.GPP3-0051-2018.

62. Marquis, R.E.; Clock, S.A.; Mota-Meira, M. Fluoride and organic weak acids as modulators of microbial physiology. *FEMS Microbiol Rev* **2003**, *26*, 493-510, doi:10.1111/j.1574-6976.2003.tb00627.x.

63. Miki, S.; Kitagawa, H.; Kitagawa, R.; Kiba, W.; Hayashi, M.; Imazato, S. Antibacterial activity of resin composites containing surface pre-reacted glass-ionomer (S-PRG) filler. *Dent Mater* **2016**, *32*, 1095-1102, doi:10.1016/j.dental.2016.06.018.

3 CONCLUSÃO

Esse estudo explorou o comportamento físico-mecânico e biológico de um CIV de baixa viscosidade e de um CIV de alta viscosidade, quando da adição de Biosilicato®. Para ambos CIVs, quando o Biosilicato® foi adicionado em baixa concentração (5%) observou-se melhor qualidade superficial comparada às concentrações mais altas. No CIV de baixa viscosidade (Maxxion R), a adição de 5% de Biosilicato® agregou benefícios como elevação da liberação iônica e do potente efeito inibidor do crescimento de *S. mutans,* sem afetar as propriedades físico-mecânicas. Porém, apresentou-se como uma das concentrações mais citotóxicas.

Para o CIV de alta viscosidade (Fuji IX GP), observou-se diminuição das propriedades físico/mecânicas, não alterando a citotoxicidade do material e aumentando a liberação de íons terapêuticos (Si, P, Na, Ca e F), porém sem aumentar o efeito antimicrobiano.

REFERÊNCIAS*

1. Sidhu SK, Nicholson JW. A Review of Glass-Ionomer Cements for Clinical Dentistry. J Funct Biomater. 2016;7(3).
2. Hasan A, Sidhu SK, Nicholson JW. Fluoride release and uptake in enhanced bioactivity glass ionomer cement ("glass carbomer™") compared with conventional and resin-modified glass ionomer cements. J Appl Oral Sci. 2019;27:e20180230.
3. Šalinović I, Stunja M, Schauperl Z, Verzak Ž, Ivanišević Malčić A, Brzović Rajić V. Mechanical Properties of High Viscosity Glass Ionomer and Glass Hybrid Restorative Materials. Acta Stomatol Croat. 2019;53(2):125-31.
4. Mickenautsch S. High-viscosity glass-ionomer cements for direct posterior tooth restorations in permanent teeth: The evidence in brief. J Dent. 2016;55:121-3.
5. Hill R. Glass ionomer polyalkenoate cements and related materials: past, present and future. Br Dent J. 2022;232(9):653-7.
6. de Lima Navarro MF, Pascotto RC, Borges AFS, Soares CJ, Raggio DP, Rios D, et al. Consensus on glass-ionomer cement thresholds for restorative indications. J Dent. 2021;107:103609.
7. Garcez RM, Buzalaf MA, de Araújo PA. Fluoride release of six restorative materials in water and pH-cycling solutions. J Appl Oral Sci. 2007;15(5):406-11.
8. Alhalawani AM, Curran DJ, Boyd D, Towler MR. The role of poly (acrylic acid) in conventional glass polyalkenoate cements. Journal of Polymer Engineering. 2016;36(3):221-37.
9. Nicholson J. Glass-ionomer cements for clinical dentistry. Mater Technol. 2010;25:8-13.
10. Moshaverinia A, Roohpour N, Chee WW, Schricker SR. A review of powder modifications in conventional glass-ionomer dental cements. Journal of materials chemistry. 2011;21(5):1319-28.
11. Abbasi R, Nodehi A, Atai M. Synthesis of poly(acrylic-co-itaconic acid) through precipitation photopolymerization for glass-ionomer cements: Characterization and properties of the cements. Dent Mater. 2020;36(6):e169-e83.

* De acordo com as normas da UNICAMP/FOP, baseadas na padronização do International Committee of Medical Journal Editors - Vancouver Group. Abreviatura dos periódicos em conformidade com o PubMed.

12. Howard L, Weng Y, Xie D. Preparation and evaluation of a novel star-shaped polyacid-constructed dental glass-ionomer system. Dent Mater. 2014;30(6):644-53.
13. Wetzel R, Eckardt O, Biehl P, Brauer DS, Schacher FH. Effect of poly(acrylic acid) architecture on setting and mechanical properties of glass ionomer cements. Dent Mater. 2020;36(3):377-86.
14. Crisp S, Wilson AD. Reactions in glass ionomer cements: V. Effect of incorporating tartaric acid in the cement liquid. J Dent Res. 1976;55(6):1023-31.
15. Nicholson JW. Maturation processes in glass-ionomer dental cements. Acta Biomater Odontol Scand. 2018;4(1):63-71.
16. Fuchs M, Gentleman E, Shahid S, Hill RG, Brauer DS. Therapeutic ion-releasing bioactive glass ionomer cements with improved mechanical strength and radiopacity. Frontiers in Materials. 2015:63.
17. Nicholson J, Brookman P, Lacy O, Wilson A. Fourier transform infrared spectroscopic study of the role of tartaric acid in glass-ionomer dental cements. Journal of dental research. 1988;67(12):1451-4.
18. Yamakami SA, Ubaldini ALM, Sato F, Medina Neto A, Pascotto RC, Baesso ML. Study of the chemical interaction between a high-viscosity glass ionomer cement and dentin. Journal of Applied Oral Science. 2018;26.
19. Frencken JE. The ART approach using glass-ionomers in relation to global oral health care. Dental materials. 2010;26(1):1-6.
20. Frencken JE, Pilot T, Songpaisan Y, Phantumvanit P. Atraumatic restorative treatment (ART): rationale, technique, and development. Journal of public health dentistry. 1996;56(3):135-40.
21. Menezes-Silva R, Velasco SRM, BRESCIANi E, Bastos RdS, Navarro MFdL. A prospective and randomized clinical trial evaluating the effectiveness of ART restorations with high-viscosity glass-ionomer cement versus conventional restorations with resin composite in Class II cavities of permanent teeth: two-year follow-up. Journal of applied oral science. 2021;29.
22. Moura MSd, Sousa GPd, Brito MHSF, Silva MCC, Lima MdDMd, Moura LdFAdD, et al. Does low-cost GIC have the same survival rate as high-viscosity

* De acordo com as normas da UNICAMP/FOP, baseadas na padronização do International Committee of Medical Journal Editors - Vancouver Group. Abreviatura dos periódicos em conformidade com o PubMed.

GIC in atraumatic restorative treatments? A RCT. Brazilian Oral Research. 2020;33.

23. Kim J, Vaughn RM, Gu L, Rockman RA, Arola DD, Schafer TE, et al. Imperfect hybrid layers created by an aggressive one-step self-etch adhesive in primary dentin are amendable to biomimetic remineralization in vitro. Journal of Biomedical Materials Research Part A: An Official Journal of The Society for Biomaterials, The Japanese Society for Biomaterials, and The Australian Society for Biomaterials and the Korean Society for Biomaterials. 2010;93(4):1225-34.
24. Damé-Teixeira N, Ev LD, Bitello-Firmino L, Soares VK, Dalalba RS, Rup AG, et al. Characterization of Lactobacilli isolated from carious dentin after selective caries removal and cavity sealing. Archives of Oral Biology. 2021;121:104988.
25. De Castilho ARF, Rosalen PL, de Souza Araujo IJ, Kitagawa IL, Costa CAGdA, Janal MN, et al. Trans, trans-farnesol, an antimicrobial natural compound, improves glass ionomer cement properties. Plos one. 2019;14(8):e0220718.
26. Pinto IC, Seibert JB, Pinto LS, Santos VR, de Sousa RF, Sousa LR, et al. Preparation of glass-ionomer cement containing ethanolic Brazilian pepper extract (Schinus terebinthifolius Raddi) fruits: chemical and biological assays. Scientific Reports. 2020;10(1):22312.
27. Deepalakshmi M, Poorni S, Miglani R, Rajamani I, Ramachandran S. Evaluation of the antibacterial and physical properties of glass ionomer cements containing chlorhexidine and cetrimide: an in-vitro study. Indian J Dent Res. 2010;21(4):552-6.
28. Mittal S, Soni H, Sharma DK, Mittal K, Pathania V, Sharma S. Comparative evaluation of the antibacterial and physical properties of conventional glass ionomer cement containing chlorhexidine and antibiotics. J Int Soc Prev Community Dent. 2015;5(4):268-75.
29. Takahashi Y, Imazato S, Kaneshiro AV, Ebisu S, Frencken JE, Tay FR. Antibacterial effects and physical properties of glass-ionomer cements containing chlorhexidine for the ART approach. Dental Materials. 2006;22(7):647-52.

* De acordo com as normas da UNICAMP/FOP, baseadas na padronização do International Committee of Medical Journal Editors - Vancouver Group. Abreviatura dos periódicos em conformidade com o PubMed.

30. Yadiki JV, Jampanapalli SR, Konda S, Inguva HC, Chimata VK. Comparative Evaluation of the Antimicrobial Properties of Glass Ionomer Cements with and without Chlorhexidine Gluconate. Int J Clin Pediatr Dent. 2016;9(2):99-103.
31. Araújo IJdS, Ricardo MG, Gomes OP, Giovani PA, Puppin-Rontani J, Pecorari VA, et al. Titanium dioxide nanotubes added to glass ionomer cements affect S. mutans viability and mechanisms of virulence. Brazilian Oral Research. 2021;35.
32. Ashour AA, Basha S, Felemban NH, Enan ET, Alyamani AA, Gad El-Rab SM. Antimicrobial Efficacy of Glass Ionomer Cement in Incorporation with Biogenic Zingiber officinale Capped Silver-Nanobiotic, Chlorhexidine Diacetate and Lyophilized Miswak. Molecules. 2022;27(2):528.
33. Jowkar Z, Jowkar M, Shafiei F. Mechanical and dentin bond strength properties of the nanosilver enriched glass ionomer cement. Journal of clinical and experimental dentistry. 2019;11(3):e275.
34. Paiva L, Fidalgo TKS, da Costa LP, Maia LC, Balan L, Anselme K, et al. Antibacterial properties and compressive strength of new one-step preparation silver nanoparticles in glass ionomer cements (NanoAg-GIC). J Dent. 2018;69:102-9.
35. Autefage H, Gentleman E, Littmann E, Hedegaard MA, Von Erlach T, O'Donnell M, et al. Sparse feature selection methods identify unexpected global cellular response to strontium-containing materials. Proceedings of the National Academy of Sciences. 2015;112(14):4280-5.
36. Gentleman E, Fredholm YC, Jell G, Lotfibakhshaiesh N, O'Donnell MD, Hill RG, et al. The effects of strontium-substituted bioactive glasses on osteoblasts and osteoclasts in vitro. Biomaterials. 2010;31(14):3949-56.
37. Binaljadm T, Moorehead R, Almela T, Franklin K, Tayebi L, Moharamzadeh K. Biomodification of a class-V restorative material by incorporation of bioactive agents. Dentistry Journal. 2019;7(4):110.
38. Gu Y, Yap A, Cheang P, Khor K. Effects of incorporation of HA/ZrO2 into glass ionomer cement (GIC). Biomaterials. 2005;26(7):713-20.

* De acordo com as normas da UNICAMP/FOP, baseadas na padronização do International Committee of Medical Journal Editors - Vancouver Group. Abreviatura dos periódicos em conformidade com o PubMed.

39. Lucas ME, Arita K, Nishino M. Toughness, bonding and fluoride-release properties of hydroxyapatite-added glass ionomer cement. Biomaterials. 2003;24(21):3787-94.
40. Moshaverinia A, Ansari S, Moshaverinia M, Roohpour N, Darr JA, Rehman I. Effects of incorporation of hydroxyapatite and fluoroapatite nanobioceramics into conventional glass ionomer cements (GIC). Acta biomaterialia. 2008;4(2):432-40.
41. Nicholson J, Hawkins S, Smith J. The incorporation of hydroxyapatite into glass-polyalkenoate ("glass-ionomer") cements: a preliminary study. Journal of Materials Science: Materials in Medicine. 1993;4:418-21.
42. Yli-Urpo H, Lassila LV, Närhi T, Vallittu PK. Compressive strength and surface characterization of glass ionomer cements modified by particles of bioactive glass. Dental Materials. 2005;21(3):201-9.
43. Bansal R, Tewari U, Singh P, Murthy D. Modified polyalkenoate (glass-ionomer) cement–a study. Journal of Oral Rehabilitation. 1995;22(7):533-7.
44. Dowling AH, Stamboulis A, Fleming GJ. The influence of montmorillonite clay reinforcement on the performance of a glass ionomer restorative. Journal of Dentistry. 2006;34(10):802-10.
45. De Caluwé T, Vercruysse CW, Ladik I, Convents R, Declercq H, Martens LC, et al. Addition of bioactive glass to glass ionomer cements: Effect on the physico-chemical properties and biocompatibility. Dent Mater. 2017;33(4):e186-e203.
46. Skallevold HE, Rokaya D, Khurshid Z, Zafar MS. Bioactive glass applications in dentistry. International Journal of Molecular Sciences. 2019;20(23):5960.
47. Siqueira RL, Zanotto ED. Biosilicato®: histórico de uma vitrocerâmica brasileira de elevada bioatividade. Química nova. 2011;34:1231-41.
48. Baino F. Bioactive glasses–when glass science and technology meet regenerative medicine. Ceramics International. 2018;44(13):14953-66.
49. Hench LL. An introduction to bioceramics: World scientific; 1993.
50. Forsback AP, Areva S, Salonen J. Mineralization of dentin induced by treatment with bioactive glass S53P4 in vitro. Acta Odontologica Scandinavica. 2004;62(1):14-20.

* De acordo com as normas da UNICAMP/FOP, baseadas na padronização do International Committee of Medical Journal Editors - Vancouver Group. Abreviatura dos periódicos em conformidade com o PubMed.

51. Efflandt S, Magne P, Douglas W, Francis L. Interaction between bioactive glasses and human dentin. Journal of materials science: materials in medicine. 2002;13(6):557.
52. Abuna G, Campos P, Hirashi N, Giannini M, Nikaido T, Tagami J, et al. The ability of a nanobioglass-doped self-etching adhesive to re-mineralize and bond to artificially demineralized dentin. Dental Materials. 2021;37(1):120-30.
53. Kim H-J, Bae HE, Lee J-E, Park I-S, Kim H-G, Kwon J, et al. Effects of bioactive glass incorporation into glass ionomer cement on demineralized dentin. Scientific Reports. 2021;11(1):7016.
54. Black J, Hastings G. Handbook of biomaterial properties: Springer Science & Business Media; 2013.
55. Tiskaya M, Shahid S, Gillam D, Hill R. The use of bioactive glass (BAG) in dental composites: A critical review. Dental Materials. 2021;37(2):296-310.
56. Höland W. Biocompatible and bioactive glass-ceramics—state of the art and new directions. Journal of Non-Crystalline Solids. 1997;219:192-7.
57. Hoppe A, Güldal NS, Boccaccini AR. A review of the biological response to ionic dissolution products from bioactive glasses and glass-ceramics. Biomaterials. 2011;32(11):2757-74.
58. Peitl O, Zanotto ED, Hench LL. Highly bioactive P2O5–Na2O–CaO–SiO2 glass-ceramics. Journal of Non-Crystalline Solids. 2001;292(1-3):115-26.
59. Crovace MC, Souza MT, Chinaglia CR, Peitl O, Zanotto ED. Biosilicate®—A multipurpose, highly bioactive glass-ceramic. In vitro, in vivo and clinical trials. Journal of Non-Crystalline Solids. 2016;432:90-110.
60. Nicholson JW, Sidhu SK, Czarnecka B. Enhancing the Mechanical Properties of Glass-Ionomer Dental Cements: A Review. Materials (Basel). 2020;13(11).
61. Callister WD, Rethwisch DG. Materials science and engineering: an introduction: John wiley & sons New York; 2007.
62. Tirapelli C, Panzeri H, Soares RG, Peitl O, Zanotto ED. A novel bioactive glass-ceramic for treating dentin hypersensitivity. Braz Oral Res. 2010;24(4):381-7.
63. Moura J, Teixeira LN, Ravagnani C, Peitl O, Zanotto ED, Beloti MM, et al. In vitro osteogenesis on a highly bioactive glass-ceramic (Biosilicate). J Biomed Mater Res A. 2007;82(3):545-57.

* De acordo com as normas da UNICAMP/FOP, baseadas na padronização do International Committee of Medical Journal Editors - Vancouver Group. Abreviatura dos periódicos em conformidade com o PubMed.

64. Carminatti M, Benetti F, Siqueira RL, Zanotto ED, Briso ALF, Chaves-Neto AH, et al. Experimental gel containing bioactive glass-ceramic to minimize the pulp damage caused by dental bleaching in rats. J Appl Oral Sci. 2020;28:e20190384.
65. Roriz VM, Rosa AL, Peitl O, Zanotto ED, Panzeri H, de Oliveira PT. Efficacy of a bioactive glass-ceramic (Biosilicate) in the maintenance of alveolar ridges and in osseointegration of titanium implants. Clin Oral Implants Res. 2010;21(2):148-55.
66. Siqueira RL, Alves PFS, da Silva Moraes T, Casemiro LA, da Silva SN, Peitl O, et al. Cation-doped bioactive ceramics: In vitro bioactivity and effect against bacteria of the oral cavity. Ceramics International. 2019;45(7):9231-44.
67. Brock TD, Madigan MT, Martinko JM, Parker J. Molecular systematics and microbial evolution. Biology of Microorganisms, 7th Edition, Prentice Hall: Englewood Cliffs, New Jersey. 1994:692-717.
68. Murray PR, Baron E, Pfaller M, Tenover F, Yolken R, Greenwood D. Manual of clinical microbiology (6th edn). Trends in Microbiology. 1996;4(2):83.

* De acordo com as normas da UNICAMP/FOP, baseadas na padronização do International Committee of Medical Journal Editors - Vancouver Group. Abreviatura dos periódicos em conformidade com o PubMed.

APÊNDICES

Apêndice 1 – Ilustração esquemática da análise de liberação iônica por ICP OES e por Espectroscopia UV-Vis.

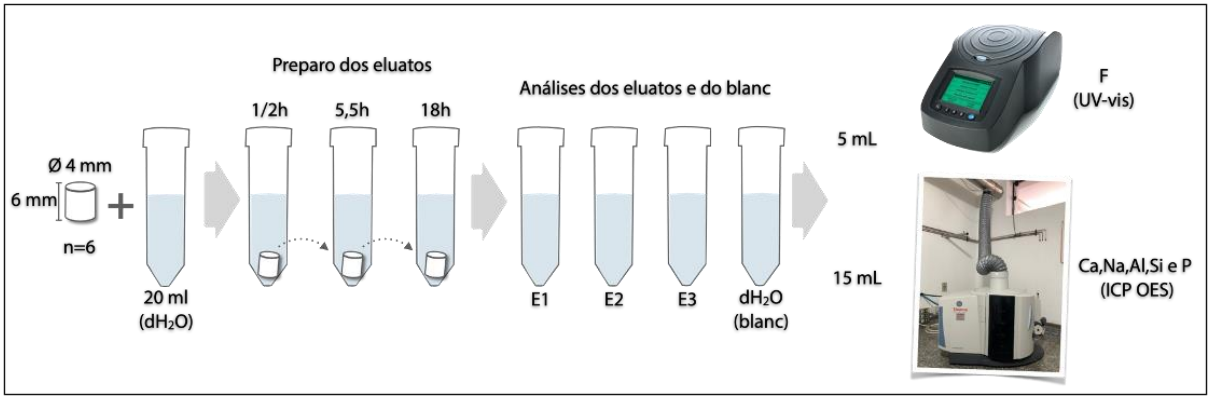

Os espécimes foram imersos em 20mL de água deionizada e após 1/2h foram transferidos para outro tubo plástico contendo água deionizada onde permaneceram por 5 horas e meia. Decorrido esse tempo, os espécimes foram transferidos novamente para outro tubo plástico com 20 mL de água deionizada e após 18 horas foram retirados. Restando 3 eluatos por espécime, correspondentes aos tempos de 1/2h (E1 – eluato 1), 5, 5h (E2 – eluato 2) e 18h (E3 – eluato 3). A determinação e quantificação iônica de flúor foi realizada por Espectroscopia UV-*Vis.* Os íons cálcio, sódio, fósforo, silício e alumínio foram determinados e quantificados por ICP OES. Os valores de quantificação de cada eluato foram normalizados de acordo com o limite de quantificação dos equipamentos para cada elemento. Após a normalização, as concentrações por elemento foram somadas, resultando na concentração cumulativa de cada elemento em 24h.

Apêndice 2 – Ilustração esquemática do teste de citotoxicidade dos CIVs.

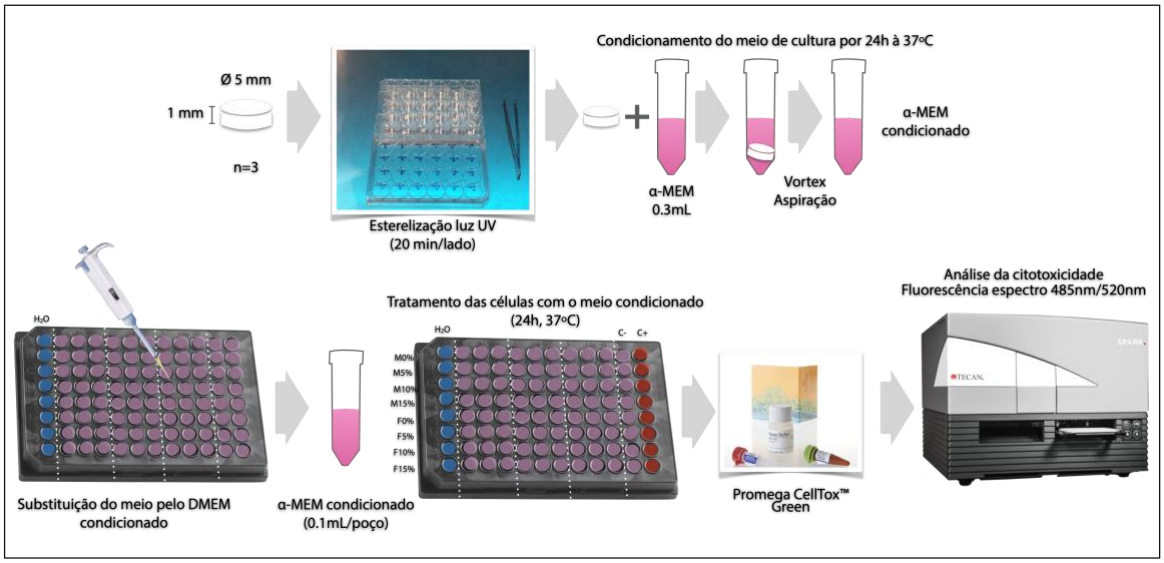

Após a confecção dos espécimes, estes foram esterilizados em luz ultravioleta por 20 minutos cada lado. Em seguida o condicionamento do meio de cultura α-MEM, feito através da imersão dos espécimes em 300μL de α-MEM. Após 24h de armazenamento à 37ºC, os tubos plásticos contendo o espécime e 300 μL de α-MEM, foram agitados e, em seguida, aspirados. Foi realizada a substituição do meio de cultura em que as células foram cultivadas, pelo meio condicionado pelos cimentos. Após 24h de armazenamento à 37ºC, o protocolo do Kit Promega CellTox Green® foi realizado conforme instruções do fabricante. As células expostas a *Lysis Buffer* (reagente citotóxico do Kit Promega), representadas pelos poços coloridos em vermellho, foram considerados o controle positivo (C+: 100% morte celular). As células expostas somente ao α-MEM representam o controle negativo (C-). Os poços da coluna 1 (coloridos em azul), foram preenchidos com água, para evitar a evaporação dos meios de cultura nos demais poços. A análise da citotoxicidade foi realizada pela análise de fluorescência pelo leitor de microplacas multimodo Spark® (Tecan, EUA) com comprimento de onda de excitação/emissão 485nm/520nm. Os dados foram reportados em porcentagem de células mortas em uma população, relativo ao controle positivo normalizado como 100%.

Apêndice 3 – Ilustração esquemática do teste de atividade antimicrobiana.

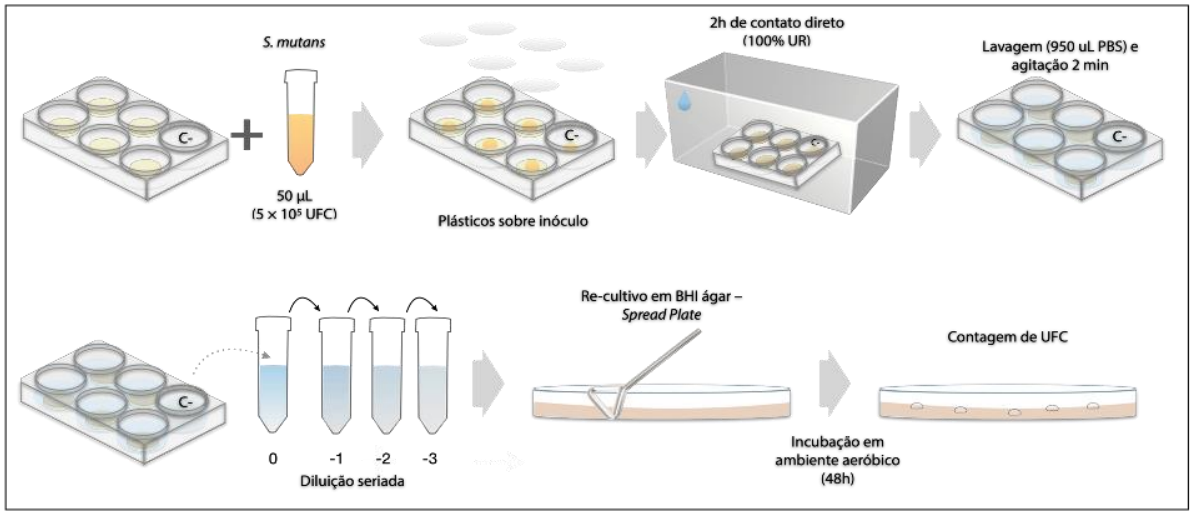

Após a esterilização dos espécimes em luz ultravioleta, os discos de CIV foram colocados em placas estéreis de 6 poços. Em seguida, 50 µL do inóculo foi colocado diretamente sobre os discos e no poço sem disco (C-). Em seguida, filmes plásticos (15 mm ø) estéreis foram colocados sobre o inóculo para garantir o espalhamento do inóculo por toda a superfície do disco. Após 2 horas de armazenamento em 100% de umidade relativa à 25°C ± 2°C, os poços foram lavados com 950 µL de PBS e agitados por 2 min (150 RPM) e uma agitadora orbital. O sobrenadante foi aspirado, e a diluição em série foi realizada. Os inóculos diluídos foram recultivados em BHI ágar, pelo método de espalhamento sobre a placa (*Spread plate*), por 48h em ambiente aeróbico. Após esse tempo a contagem de Unidades Formadoras de Colônias (UFC) foi realizada manualmente.

ANEXOS

Anexo 1 – Curvas de calibração Al, Ca, Na, Si e P.

Flexible Report By Sample

Author:

Published: 27/03/2023 09:23:53

Method Name: Curva Ca, Na, Si, Al, P (1)

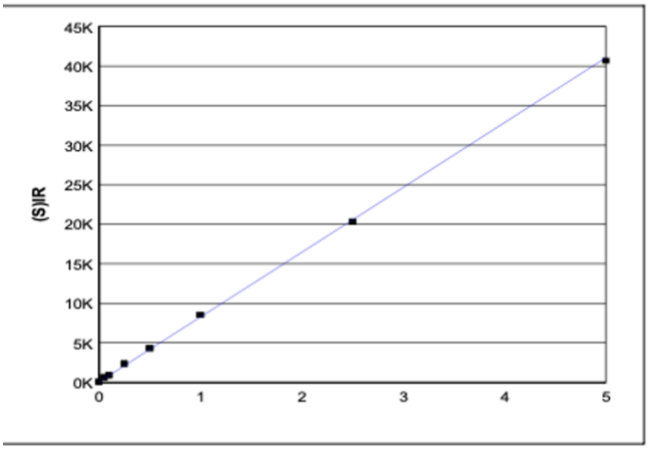

Element Name:	Al
Element Wavelength:	Al 396.152 nm
Concentration Units:	ppm
Date of Calibration:	18/07/2022 15:30:48
Date of Fit:	18/07/2022 15:30:48
Type of Fit:	Linear
Correlation:	0.9994
A0 (Offset):	121.3
A1 (Gain):	8,200
A2 (Curvature):	0.0000
n (Exponent):	1.000

Reslope		**QC Normalize**	
Slope:	1.000	**Slope factor:**	1.000
Y Int:	0.0000	**Offset:**	0.0000

Standard Name	Stated	Found	Diff	% Diff	(S)IR	Stddev	Emphasis
Blank	0.0000	-0.00002215	-0.00002215	0.0000	121.2	5.214	1
P1	0.05000	0.06520	0.01520	30.40	655.9	5.559	1
P2	0.1000	0.09872	-0.001277	-1.277	930.8	16.23	1
P3	0.2500	0.2782	0.02824	11.30	2,403	10.38	1
P4	0.5000	0.5168	0.01683	3.367	4,359	18.08	1
P5	1.000	1.030	0.03025	3.025	8,569	9.027	1
P6	2.500	2.464	-0.03644	-1.457	20,322	109.8	1
P7	5.000	4.947	-0.05281	-1.056	40,687	129.6	1

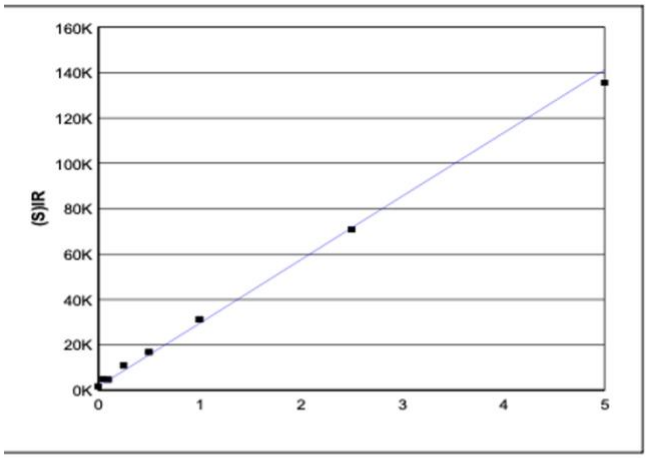

Element Name:	Ca
Element Wavelength:	Ca 393.366 nm
Concentration Units:	ppm
Date of Calibration:	18/07/2022 15:30:48
Date of Fit:	18/07/2022 15:30:48
Type of Fit:	Linear
Correlation:	0.9939
A0 (Offset):	1,718
A1 (Gain):	27,952
A2 (Curvature):	0.0000
n (Exponent):	1.000

Reslope		**QC Normalize**	
Slope:	1.000	**Slope factor:**	1.000
Y Int:	0.0000	**Offset:**	0.0000

Standard Name	Stated	Found	Diff	% Diff	(S)IR	Stddev	Emphasis
Blank	0.0000	-0.00008376	-0.00008376	0.0000	1,715	23.47	1
P1	0.05000	0.1110	0.06097	121.9	4,820	91.71	1
P2	0.1000	0.1062	0.006221	6.221	4,687	14.81	1
P3	0.2500	0.3291	0.07910	31.64	10,917	16.15	1
P4	0.5000	0.5384	0.03842	7.685	16,768	22.58	1
P5	1.000	1.054	0.05359	5.359	31,168	54.27	1
P6	2.500	2.472	-0.02775	-1.110	70,823	45.43	1
P7	5.000	4.789	-0.2105	-4.211	135,595	87.81	1

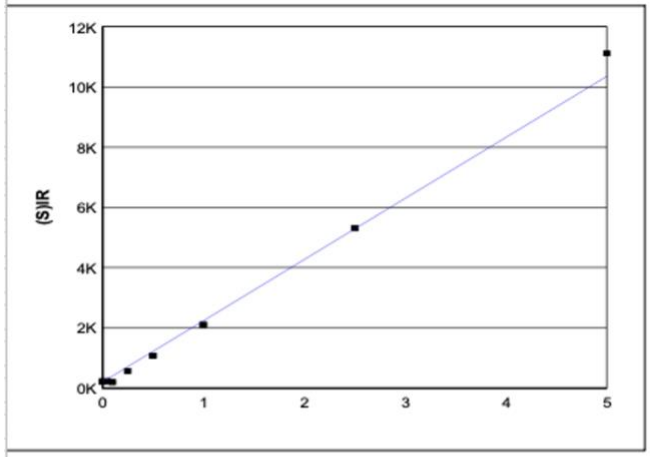

Element Name:	Na
Element Wavelength:	Na 588.995 nm
Concentration Units:	ppm
Date of Calibration:	18/07/2022 15:30:48
Date of Fit:	18/07/2022 15:30:48
Type of Fit:	Linear
Correlation:	0.9881
A0 (Offset):	219.6
A1 (Gain):	2,030
A2 (Curvature):	0.0000
n (Exponent):	1.000

Reslope		**QC Normalize**	
Slope:	1.000	**Slope factor:**	1.000
Y Int:	0.0000	**Offset:**	0.0000

Standard Name	Stated	Found	Diff	% Diff	(S)IR	Stddev	Emphasis
Blank	0.0000	0.0001225	0.0001225	0.0000	219.8	10.96	1
P1	0.05000	0.004872	-0.04513	-90.26	229.4	13.52	1
P2	0.1000	-0.009725	-0.1097	-109.7	199.8	14.62	1
P3	0.2500	0.1735	-0.07649	-30.59	571.9	9.198	1
P4	0.5000	0.4236	-0.07641	-15.28	1,080	29.84	1
P5	1.000	0.9306	-0.06939	-6.939	2,109	6.063	1
P6	2.500	2.508	0.008331	0.3332	5,313	49.03	1
P7	5.000	5.369	0.3688	7.376	11,121	29.75	1

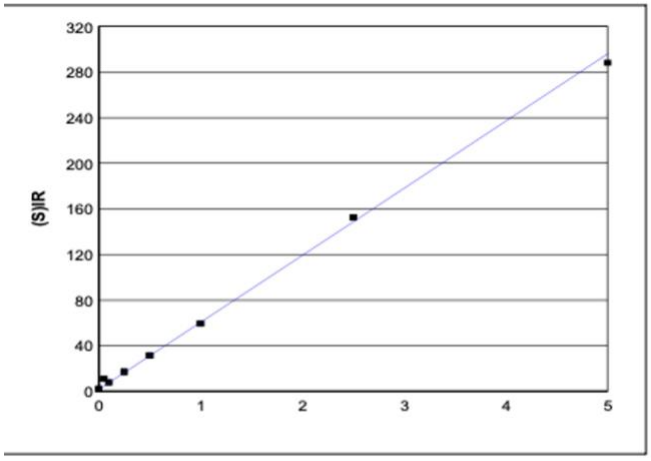

Element Name:	P
Element Wavelength:	P 177.495 nm
Concentration Units:	ppm
Date of Calibration:	18/07/2022 15:30:48
Date of Fit:	18/07/2022 15:30:48
Type of Fit:	Linear
Correlation:	0.9891
A0 (Offset):	1.970
A1 (Gain):	58.84
A2 (Curvature):	0.0000
n (Exponent):	1.000

Reslope		**QC Normalize**	
Slope:	1.000	**Slope factor:**	1.000
Y Int:	0.0000	**Offset:**	0.0000

Standard Name	Stated	Found	Diff	% Diff	(S)IR	Stddev	Emphasis
Blank	0.0000	-0.00009894	-0.00009894	0.0000	1.964	0.3451	1
P1	0.05000	0.1505	0.1005	201.0	10.83	0.3855	1
P2	0.1000	0.09771	-0.002288	-2.288	7.720	0.2290	1
P3	0.2500	0.2553	0.005267	2.107	16.99	0.2161	1
P4	0.5000	0.5000	-0.000006819	-0.001364	31.39	0.3936	1
P5	1.000	0.9744	-0.02563	-2.563	59.30	0.5405	1
P6	2.500	2.558	0.05806	2.322	152.5	0.1061	1
P7	5.000	4.864	-0.1359	-2.718	288.2	0.8431	1

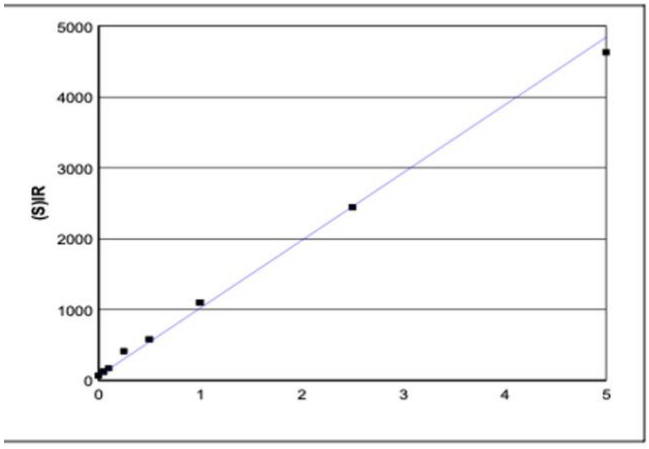

Element Name:	Si
Element Wavelength:	Si 251.611 nm
Concentration Units:	ppm
Date of Calibration:	18/07/2022 15:30:48
Date of Fit:	18/07/2022 15:30:48
Type of Fit:	Linear
Correlation:	0.9964
A0 (Offset):	67.97
A1 (Gain):	955.7
A2 (Curvature):	0.0000
n (Exponent):	1.000

Reslope		**QC Normalize**	
Slope:	1.000	**Slope factor:**	1.000
Y Int:	0.0000	**Offset:**	0.0000

Standard Name	Stated	Found	Diff	% Diff	(S)IR	Stddev	Emphasis
Blank	0.0000	-0.00003856	-0.00003856	0.0000	67.93	7.367	1
P1	0.05000	0.05774	0.007740	15.48	123.2	4.967	1
P2	0.1000	0.1083	0.008287	8.287	171.5	1.628	1
P3	0.2500	0.3590	0.1090	43.59	411.0	127.1	1
P4	0.5000	0.5345	0.03454	6.908	578.8	1.710	1
P5	1.000	1.078	0.07818	7.818	1,098	5.347	1
P6	2.500	2.489	-0.01114	-0.4457	2,447	7.113	1
P7	5.000	4.773	-0.2266	-4.532	4,630	4.349	1

Anexo 2 – Curva de calibração do fluoreto por Espectrometria Uv-Vis (método SPANDS).

Pontos	Concentração (mg/L)	Absorbância	mg Fluoreto/L (Calculado)
Branco	0.000	3.083	0.000
P1	0.100	3.023	0.121
P2	0.250	2.970	0.227
P3	0.500	2.842	0.485
P4	1.000	2.587	1.000

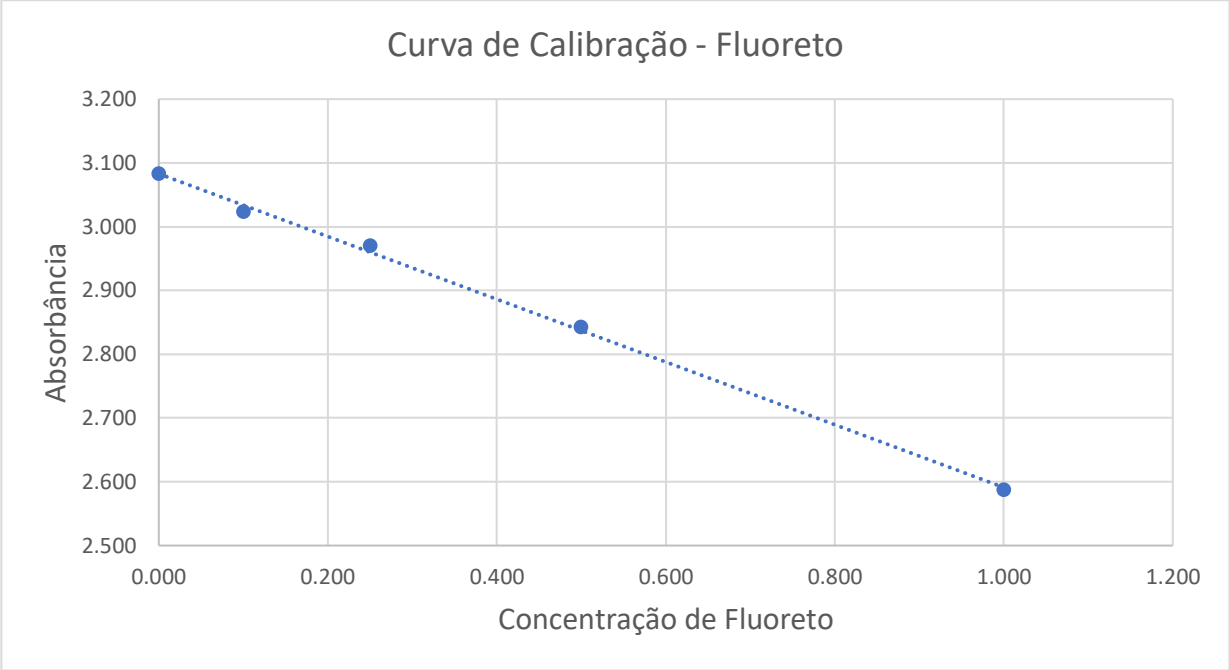

ANEXOS

Anexo 3 – Relatório de similaridade

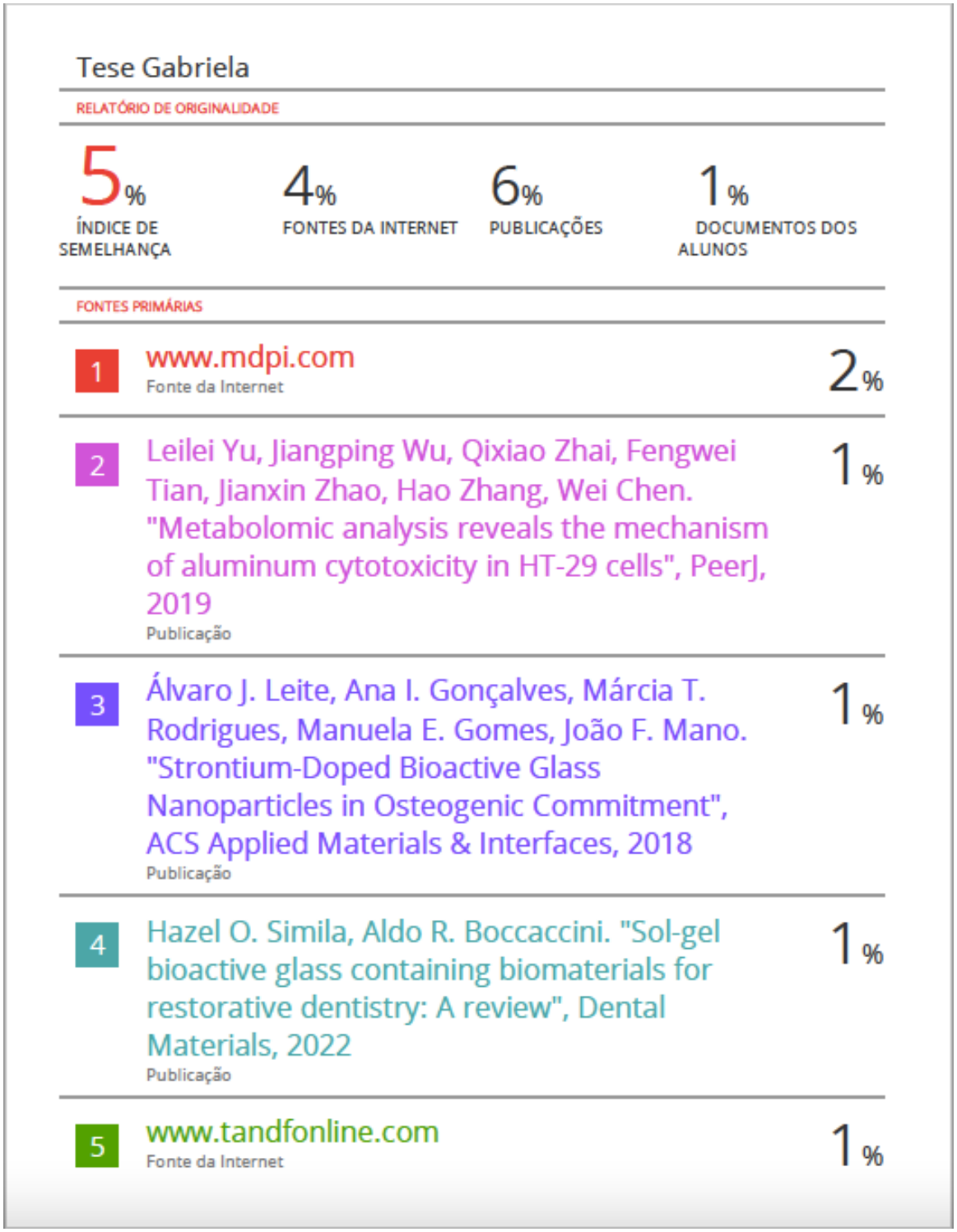

Tese Gabriela

RELATÓRIO DE ORIGINALIDADE

5%	4%	6%	1%
ÍNDICE DE SEMELHANÇA	FONTES DA INTERNET	PUBLICAÇÕES	DOCUMENTOS DOS ALUNOS

FONTES PRIMÁRIAS

1	www.mdpi.com Fonte da Internet	2%
2	Leilei Yu, Jiangping Wu, Qixiao Zhai, Fengwei Tian, Jianxin Zhao, Hao Zhang, Wei Chen. "Metabolomic analysis reveals the mechanism of aluminum cytotoxicity in HT-29 cells", PeerJ, 2019 Publicação	1%
3	Álvaro J. Leite, Ana I. Gonçalves, Márcia T. Rodrigues, Manuela E. Gomes, João F. Mano. "Strontium-Doped Bioactive Glass Nanoparticles in Osteogenic Commitment", ACS Applied Materials & Interfaces, 2018 Publicação	1%
4	Hazel O. Simila, Aldo R. Boccaccini. "Sol-gel bioactive glass containing biomaterials for restorative dentistry: A review", Dental Materials, 2022 Publicação	1%
5	www.tandfonline.com Fonte da Internet	1%

6	bonndoc.ulb.uni-bonn.de Fonte da Internet	1 %

Excluir citações	Desligado	Excluir correspondências	< 1%
Excluir bibliografia	Em		

ANEXOS

Anexo 4 – Comprovante de submissão do artigo.

[JFB] Manuscript ID: jfb-2340829 - Submission Received Caixa de entrada ×

Editorial Office <jfb@mdpi.com> ter., 28 de mar., 08:23

para mim, Joshua, Cristine, Laura, Rafael, Marina, Edgar, And

inglês > português Traduzir mensagem Desativar para:

Dear Dr. Magalhães,

Thank you very much for uploading the following manuscript to the MDPI submission system. One of our editors will be in touch with you soon.

Journal name: Journal of Functional Biomaterials
Manuscript ID: jfb-2340829
Type of manuscript: Article
Title: Effect of Biosilicate® addition on the physical-mechanical and biological properties of dental glass ionomer cements.
Authors: Gabriela De Alencar Pinto Magalhães, Joshua J. Thomson, Cristine Smoczer, Laura Young, Rafael Rocha Pacheco, Marina Trevelin Souza, Edgar Dutra Zanotto, And Regina M. Puppin-Rontani *
Received: 28 March 2023
E-mails: gabrielaapmag@gmail.com, thomsojo@udmercy.edu, smoczecr@udmercy.edu, youngla3@udmercy.edu, rapacheco@augusta.edu, marina.trevelin@gmail.com, dedz@ufscar.br, rmpuppin@unicamp.br
Submitted to section: Dental Biomaterials, https://www.mdpi.com/journal/jfb/sections/dental_biomaterials
Functional Materials for Dental Restorations
https://www.mdpi.com/journal/jfb/special_issues/8NG2NB904S